Fermi National Accelerator Laboratory

Alignment Tolerances of IR Quadrupoles in the LHC

Tanaji Sen

Fermi National Accelerator Laboratory
P.O. Box 500, Batavia, Illinois 60510

November 1999

Disclaimer

This report was prepared as an account of work sponsored by an agency of the United States Government. Neither the United States Government nor any agency thereof, nor any of their employees, makes any warranty, expressed or implied, or assumes any legal liability or responsibility for the accuracy, completeness, or usefulness of any information, apparatus, product, or process disclosed, or represents that its use would not infringe privately owned rights. Reference herein to any specific commercial product, process, or service by trade name, trademark, manufacturer, or otherwise, does not necessarily constitute or imply its endorsement, recommendation, or favoring by the United States Government or any agency thereof. The views and opinions of authors expressed herein do not necessarily state or reflect those of the United States Government or any agency thereof.

Distribution

Approved for public release; further dissemination unlimited.

Copyright Notification

This manuscript has been authored by Universities Research Association, Inc. under contract No. DE-AC02-76CH03000 with the U.S. Department of Energy. The United States Government and the publisher, by accepting the article for publication, acknowledges that the United States Government retains a nonexclusive, paid-up, irrevocable, worldwide license to publish or reproduce the published form of this manuscript, or allow others to do so, for United States Government Purposes.

Alignment Tolerances of IR Quadrupoles in the LHC

Tanaji Sen
FNAL
Batavia, IL 60510

Contents

1   Introduction

Luminosity in the LHC will depend critically on the alignment of the triplet quadrupoles. These quadrupoles are closest to the interaction points (IPs), have large gradients and the β functions have their largest values within these quadrupoles. Within a triplet, the cold masses of the Q1 and Q3 quadrupoles will be housed in separate cryostats while Q2a and Q2b will be placed in a single cryostat. The absolute alignments of Q1, Q3 and the Q2a/Q2b pair with respect to the desired axes will be determined during installation. The relative alignment of Q2a and Q2b however will be fixed once they are placed in their common cryostat at Fermilab. In this note, we examine the required relative alignment tolerances of Q2a and Q2b. An early study of some alignment tolerances was done by Weisz [1].

1.1   Criteria for estimating alignment tolerances

The most important criterion is that the misalignments should not affect the luminosity significantly. Aperture and beam stability also place constraints on the allowed misalignments. Below we list in more detail some of the parameters which must be kept nearly invariant.

- Minimal effect on luminosity

  - Separation between the beams at the IPs should be small.
  - Change in β^* should be small.
  - Dispersion at the IP should be small, both for maximum luminosity and avoiding synchro-betatron resonances.

- Physical aperture must be preserved.

- Dynamic aperture must be preserved.

- Long-range beam-beam interactions should not be enhanced so the separation between the beams should be preserved.

- Minimal changes to the linear optics - coupling, β beat, tune shift. The most important of these is the coupling.

- Head-on beam-beam tune shifts should not increase, so there should be little change in the beam sizes at the IPs. For round beams, these tune shifts are independent of β^*. However misalignment errors may change the aspect ratio in which case these tune shifts do depend on β^*.

The effect of a quadrupole misalignment depends on the degree of freedom that is misaligned. Table 1 shows the effects of rigid modes of misalignments in the six degrees of freedom on the beam optics. Non-rigid modes such as variations in straightness or sag and twist can also occur due to construction errors. These can be modelled as changes in the rigid misalignment along the length of a magnet. Experience with the model magnets built so far at Fermilab shows that these non-rigid misalignments are very small [2]. The magnitude of the impact depends on the beta function in the

Misalignment	Effect on the optics
Transverse displacements	Orbit shift
	Tune shift (with nonlinear magnets)
Longitudinal displacement	Tune shift, beta beat, dispersion beat
Pitch and Yaw	Orbit shift
	Tune shift (with nonlinear magnets)
Roll	Enhanced coupling, orbit shift(with crossing angle)
	Beta beat, dispersion beat

Table 1: Rigid misalignments of quadrupoles and their effects on the beam optics.

quadrupole. In this report we have used LHC lattice V5.1. The table in Appendix A shows the beta functions in the two planes at various locations within the quadrupoles. These were calculated using MAD [3].

2 Transverse displacement errors

If a thin quadrupole is displaced in one of the transverse planes by Δz_q ($z = x$ or $z = y$), then particles experience a kick in the same plane and the orbit error at s is

$$z_{shift}(s) = \frac{B'L}{(B\rho)}\Delta z_q \frac{\sqrt{\beta_z(s)\beta_{z,q}}}{2\sin\pi\nu}\cos[|\psi(s) - \psi_0| - \pi\nu] = \frac{\Delta z_q}{F}\frac{\sqrt{\beta_z(s)\beta_{z,q}}}{2\sin\pi\nu}\cos[|\psi(s) - \psi_0| - \pi\nu] \quad (1)$$

The inverse focal length of the displaced quadrupole is $1/F = B'L/(B\rho)$ and $\beta_{z,q}$ is the beta function at the location of the quadrupole. The phase advance from the high-beta quadrupoles to the nearest IP is very close to $90°$. In the middle of a focusing Q2b magnet, $\beta_{z,q} = 4567$m while $B'/(B\rho) = 0.858 \times 10^{-2}$ m^{-2}, $L = 5.5$m. Hence the orbit displacement at the IP per unit displacement of Q2b in the focusing plane is

$$\frac{z_{shift,IP}}{\Delta z_q} = 1.13 \quad (2)$$

This agrees well with a MAD calculation which gives 1.10 for the same ratio. Thus a displacement of Q2b by 1mm leads to an orbit shift of 1.10mm at the IP, which is very large when measured in units of the rms beam size at the IP.

2.1 Effect on the luminosity without error correction

Figure 1: Relative displacement between the beams at an IP
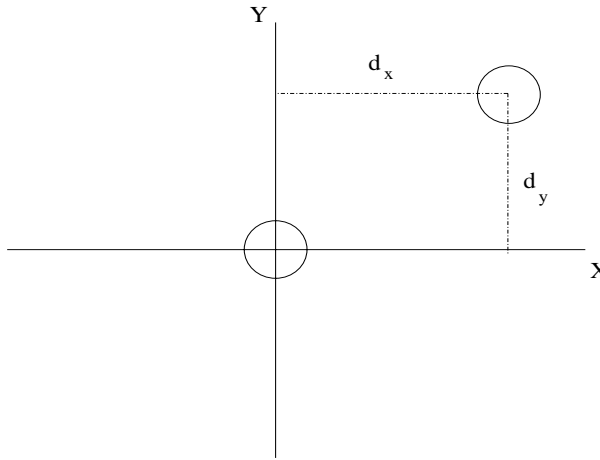
The nominal luminosity for perfectly centered beams with Gaussian density distributions is

$$\mathcal{L}_0 = \frac{f_{rev}M_B N_1 N_2}{2\pi}\frac{R_{XA}}{\sqrt{\sigma_{x,1}^2 + \sigma_{x,2}^2}\sqrt{\sigma_{y,1}^2 + \sigma_{y,2}^2}} \quad (3)$$

f_{rev} is the revolution frequency, M_B is the number of bunches, N_1, N_2 are the number of particles per bunch in the two beams. R_{XA}, the luminosity reduction factor due to the crossing angle, is given by $R_{XA} = 1/\sqrt{1 + (\phi\sigma_s/\sigma_\perp)^2}$. In this expression, ϕ is half the crossing angle, σ_s is the rms longitudinal bunch length and $\sigma_\perp$ is the rms transverse beam size in the plane of the crossing angle. If there is an offset between the two beams of (d_x, d_y) in the horizontal and vertical planes, then the luminosity drops to

$$\mathcal{L} = \mathcal{L}_0 \exp[-\frac{d_x^2}{2(\sigma_{x,1}^2 + \sigma_{x,2}^2)}]\exp[-\frac{d_y^2}{2(\sigma_{y,1}^2 + \sigma_{y,2}^2)}] \quad (4)$$

The two beams will be kicked in opposite directions by the displacement of the quadrupole Δz_q. The orbit shift of beam 2 at the IP due to a displacement in Q2b is given by $z_{shift,2}(IP) = -\sqrt{\beta_{z,q,2}/\beta_{z,q,1}}z_{shift,1}(IP) = -0.7\Delta z_q$, where $\beta_{z,q,2}$ is the beta function of beam 2 at the location of Q2b. The offset between the beams at the IP is $d_z = z_{shift,1}(IP) + |z_{shift,2}(IP)| = 1.83\Delta z_q$.

Assuming that the quadrupole is displaced in a single plane, the relative luminosity is

$$\frac{\mathcal{L}}{\mathcal{L}_0} = \exp[-\frac{1}{2}\frac{d_z^2}{\sigma_{z,1}^2 + \sigma_{z,2}^2}] = \exp[-0.84(\frac{\Delta z_q}{\sigma_z})^2] \quad (5)$$

Requiring that the relative luminosity be greater than 0.98 implies

$$\frac{\Delta z_q}{\sigma_z} \leq 0.16 \quad (6)$$

Since the beam size at the IP is 15.85μm, the misalignment of the Q2b quadrupole must be less than 2.5μm if no orbit correction is done in order to limit the luminosity loss to less than 2%.
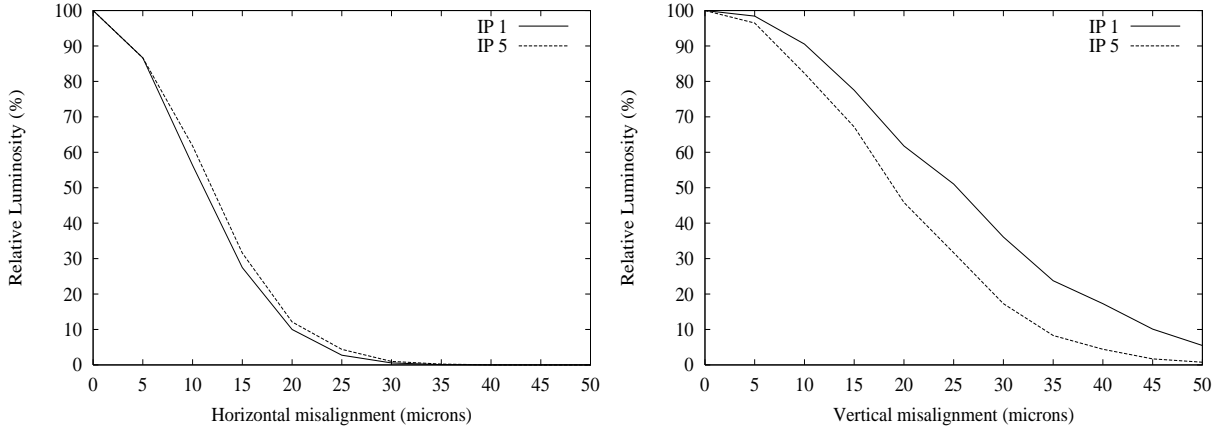
Figure 2: Relative luminosity due to a horizontal misalignment (left) and vertical misalignment (right) of Q2b. No orbit corrections.

Figure 2 shows the relative luminosity at both IP1 and IP5 as a function of the transverse misalignment of only a single Q2b in IR5. The relative luminosity was calculated using Equation (4) and the displacements d_x, d_y at the IPs were obtained with MAD. β_x in the displaced quadrupole is larger than β_y so the horizontal luminosity falls faster with increasing displacement. This figure also shows that an uncorrected transverse misalignment of $\sim 25\mu$ will be sufficient to reduce the luminosity to nearly zero.
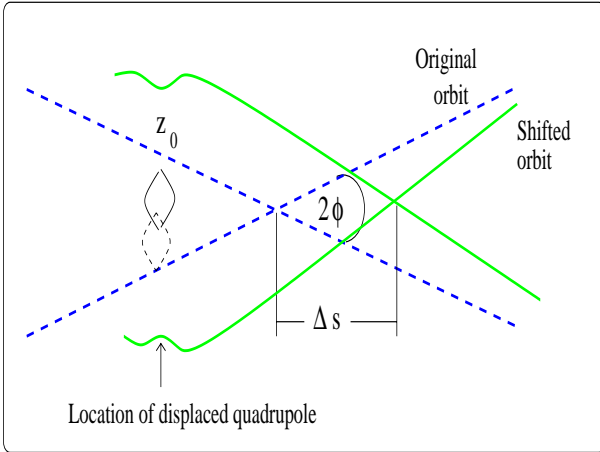

Figure 3: Longitudinal shift of the IP due to an orbit shift in the crossing plane.

We have assumed above that the IP cannot be allowed to shift longitudinally while preserving the luminosity. If a certain amount of longitudinal shift is allowed, then as Figure 3 shows, the beams do collide again at another point provided the quadrupole offset is in the crossing plane. The location of the new IP is the solution of the equation $z_0(s) + z_{shift}(s) = 0$ [1] where z_0 is the location of the closed orbit without misalignments and z_{shift} is the shift in the closed orbit given by Equation (1). Assuming that the misalignment is small enough so that the shifted IP is in the drift space, the distance Δs of the new IP from the old IP is given by the solution of the transcendental equation

$$\phi\Delta s + \frac{\Delta z_q}{2F}\sqrt{[\beta^* + \frac{\Delta s^2}{\beta^*}]\beta_{z,q}}\frac{\cos[\Delta\psi - \pi\nu]}{\sin \pi\nu} = 0 \quad (7)$$

where $\Delta\psi$ is the phase advance from the displaced quadrupole to the new IP. This equation can be solved in an iterative process to the desired accuracy. As a first approximation we can assume that the shifted IP is close enough to the old IP so that $\Delta\psi \approx \pi/2$. The first order solution is

$$\Delta s = \pm\frac{\Delta z_q}{2F}\left[\frac{\beta_{z,q}\beta^*}{\phi^2 - (\frac{\Delta z_q}{2F})^2\frac{\beta_{z,q}}{\beta^*}}\right]^{1/2} \quad (8)$$

This equation also implies that there is an upper bound to the quadrupole displacement beyond which the beams do not

---

[1]Here we have assumed that the collision occurs at $z = 0$. If desired, this can be replaced by the more exact equation $[z_0(s) + z_{shift}(s)]_1 = [z_0(s) + z_{shift}(s)]_2$ where the subscripts specify the two beams.

collide at a shifted IP. The maximum quadrupole displacement is

$$\Delta z_{q,max} = \pm [\frac{\beta^*}{\beta_{z,q}}]^{1/2} \phi(2F) \tag{9}$$

Substituting the values for Q2b, i.e. $F = 21.19$m, $\beta_{z,q} = 4567$m and $\phi = 150$ μrad, the maximum displacement which still gives a collision point is

$$\Delta z_{q,max}(Q2b) = \pm 67 \ \mu m \tag{10}$$

This tolerance is somewhat more relaxed than that obtained above where the IP was not allowed to shift longitudinally. For displacements $\Delta z_q \leq \Delta z_{q,max}$, Equation (8) can be used to estimate the longitudinal shift. For example with Δz_q (Q2b)=10μm, we find that the IP shifts by $\Delta s = 7.6$cm. To improve on this estimate, the phase advance $\Delta\psi$ from the quadrupole to this point can be calculated, substituted into Equation (7) and the new value of Δs found. This can be repeated until convergence is achieved. In any event, we find that a transverse offset of 10μm shifts the IP longitudinally by less than 10cm. The change in β^* at this location is between 1-2cm which is small compared to $\beta^* = 50$cm. The rms bunch length is 7.7cm while constraints from the experimental detectors require that the longitudinal position of the IP should shift by less than 5cm [4]. Hence a useful upper limit on the transverse misalignment of Q2b in the plane of the crossing angle is about 7μm.

If instead the quadrupole offset is in a plane transverse to the crossing plane, then the orbit in that plane will return to zero at a location where the phase advance from the displaced quadrupole satisfies $\Delta\psi = \frac{\pi}{2} + \pi\nu$. However at this location the beams will not collide as they will be offset in the crossing plane. Hence this criterion cannot be used to relax the alignment tolerance along the direction orthogonal to the crossing plane.

Dispersion at the IP affects the luminosity by changing the beam size. A non-zero horizontal dispersion D_x results in an effective horizontal rms beam size $\sigma_{x,eff} = \sqrt{\sigma_x^2 + (D_x\delta)^2}$ where δ is the rms momentum deviation. Assuming equal beam sizes for both beams, the luminosity with dispersion $\mathcal{L}(D_x)$ is related to the nominal luminosity as

$$\mathcal{L}(D_x) = \frac{\sigma_x}{\sqrt{\sigma_x^2 + (D_x\delta)^2}} \mathcal{L}_0 \tag{11}$$

With $\sigma_x = 0.01585$mm, $\delta = 1.1 \times 10^{-4}$, demanding that the relative luminosity be greater than 0.98 implies

$$D_x(\text{IP}) \leq 29 \ \text{mm} \tag{12}$$
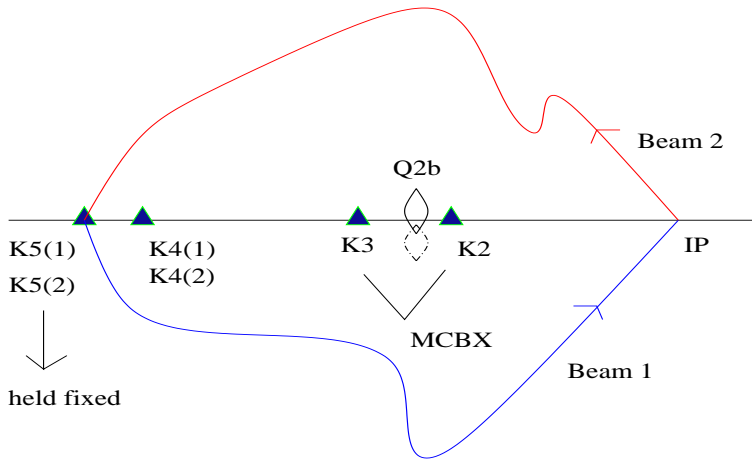
2.2 Orbit Correction

Figure 4: The desired closed orbit of both beams through the IR with Q2b misaligned. Also shown are the dipole correctors which can correct the orbit. In this paper only the correctors K2 and K3 (in the MCBX packages) and K4(1) and K4(2) are used to correct for the misalignment.

We have seen that even tiny misalignments lead to a large drop in the luminosity so the orbit shift due to the misalignment has to be corrected. The orbit offset at the IP and the closed orbit through this section of the IR can be corrected with the available dipole correctors. The crossing angles are generated with the help of two pairs of correctors, KX.Q5 and KX.Q4, one such pair acting only on a single beam. These kicks are at about 95° from the IP in the LHC lattice version 5.1. There are also dipole windings in the MCBX corrector packages which can be used to act on both beams at once.

In order to correct the orbit of both beams in MAD, we create a crossing angle in both planes at the IP using the crossing angle dipoles KX.Q5 and KX.Q4 in both planes. Due to the anti-symmetry of the optics, the x, y orbits of a single beam can be considered to represent the orbits in a single plane of both beams [1].

5

When the quadrupoles are misaligned, we need to correct the position and slope at a given point for both beams leading to 4 conditions which can be satisfied with the use of 4 correctors. The correctors KX.Q5 are already close to their maximum strengths so instead we will use the correctors KX.Q4(1), KX.Q4(2) (to be labelled K4(1), K4(2) in the sequel) and the correctors labelled K2 and K3. A sketch of the closed orbit of the two beams and the correctors is shown in Figure 4. It is worth noting that the orbit correction scheme used during operation of the LHC may differ from this scheme but we use this method as a consistent way of estimating the alignment tolerances.

In Figure 5 we show three possible ways the common cryostat can be aligned with respect to the common magnetic center of Q1 and Q3 which are assumed to be aligned for this study. Figure 6 shows that if only quadrupole Q2b is misaligned, then the maximum misalignment that can be corrected is about 0.55mm. At this value, the strength of the dipole correctors in MCBX reach their maximum values. However in practice the maximum misalignment of Q2b that can be corrected in this configuration is less since the other quadrupoles may also be misaligned. Assuming that the errors of the four quadrupoles in each triplet are uncorrelated, the misalignment tolerance is closer to $0.55/\sqrt{4}$=0.27mm.

The second case we studied was with Q2a deliberately misaligned to compensate the orbit shift due to the misalignment of Q2b. These two quadrupoles are powered with the same sign so if they are offset from the common magnetic axis in opposite directions, they will kick the beam in opposite directions and can therefore cancel each other out. The required misalignment of Q2a is determined by the beta functions at the two quadrupoles. Upstream of the IP,

$$\frac{\Delta x_{2a}}{\Delta x_{2b}} = \sqrt{\frac{\beta_{x,2b}}{\beta_{x,2a}}} = 1.05, \quad \frac{\Delta y_{2a}}{\Delta y_{2b}} = \sqrt{\frac{\beta_{y,2b}}{\beta_{y,2a}}} = 1.22 \tag{13}$$

where $(\Delta x_{2a}, \Delta x_{2b})$ are the horizontal misalignments of Q2a and Q2b respectively from the magnetic centers of the other quadrupoles and the beta functions are the values in the middle of the quadrupoles. Downstream of the IP, these ratios are interchanged due to the anti-symmetry of the optics. A study with MAD showed that the optimum settings are very close to the above expected values. Figure 7 shows the corrector strengths as a function of the relative misalignment $(\Delta x_{2a} + \Delta x_{2b})$ between the two quadrupoles. It is clear that even up to misalignment of 1mm, the required corrector strengths are very small. Figure 8 shows the orbit through the IR, first when only Q2b is misaligned by 0.5mm, and second when both Q2b and Q2a are off-axis with a relative misalignment between them of 1mm. The orbit in the second case is virtually the same as without misalignments. At the level of linear optics, it is therefore clear that relative misalignments of at least 1mm can be easily compensated. Figure 9 shows that the orbit separation between the two beams is also the same as without any misalignments. The long-range interactions are therefore not affected by this misalignment.

2.3 Dynamic Aperture

An orbit shift makes the particles go off-axis through the non-linear magnets which leads to additional orbit errors, field errors and tune shifts which can affect the dynamic aperture. With compensating misalignments of Q2a and Q2b, the closed orbit will be further away from the magnetic center in one magnet but closer in the other magnet. It is possible therefore that the dynamic aperture may depend on the signs of these misalignments.

The sign of the relative offsets between a pair Q2a, Q2b in a common cryostat will only be known after they are welded together. Considering both pairs in an IR, there are four possibilities for these offsets. Figure 10 shows three of these possibilities. In all cases, the closed orbit will be nearly exactly compensated. However the effects of the nonlinear fields may be slightly different. In those cases where the particles stay closer to the magnetic axis of the quadrupole where the beta functions are larger (Q2b), the effects of the nonlinear fields should be smaller. Thus the best setting for optimizing the dynamic aperture of a single beam would be one where it goes closer to the magnetic center of Q2b both upstream and downstream and the worst setting would be where it is further off-axis in Q2b than in Q2a both upstream and downstream. However both beams must be treated equally so the optimum offsets would be where the incoming beam goes closer to the center of Q2b. This is simply because Q2b (and Q2a) are focusing quadrupoles for the incoming beam and defocusing for the outgoing beam.

We have calculated the dynamic aperture for the different misalignments shown in Figure 10 using MAD. Particles are launched with initial amplitudes ranging from 1σ to 15σ in steps of 1σ. They are tracked for 1024 turns through the lattice with chromaticity correcting sextupoles in the arcs, IR quadrupole nonlinearities and appropriate misalignments of the selected quadrupoles. Aperture restrictions of ±30mm are placed in each quadrupole of the triplet in both IR1 and IR5. The dynamic aperture is taken to be the largest amplitude which stays stable over the turns tracked. This is repeated with three seeds for the random multipole errors in the IR quadrupoles. In this section, only Q2a and Q2b on
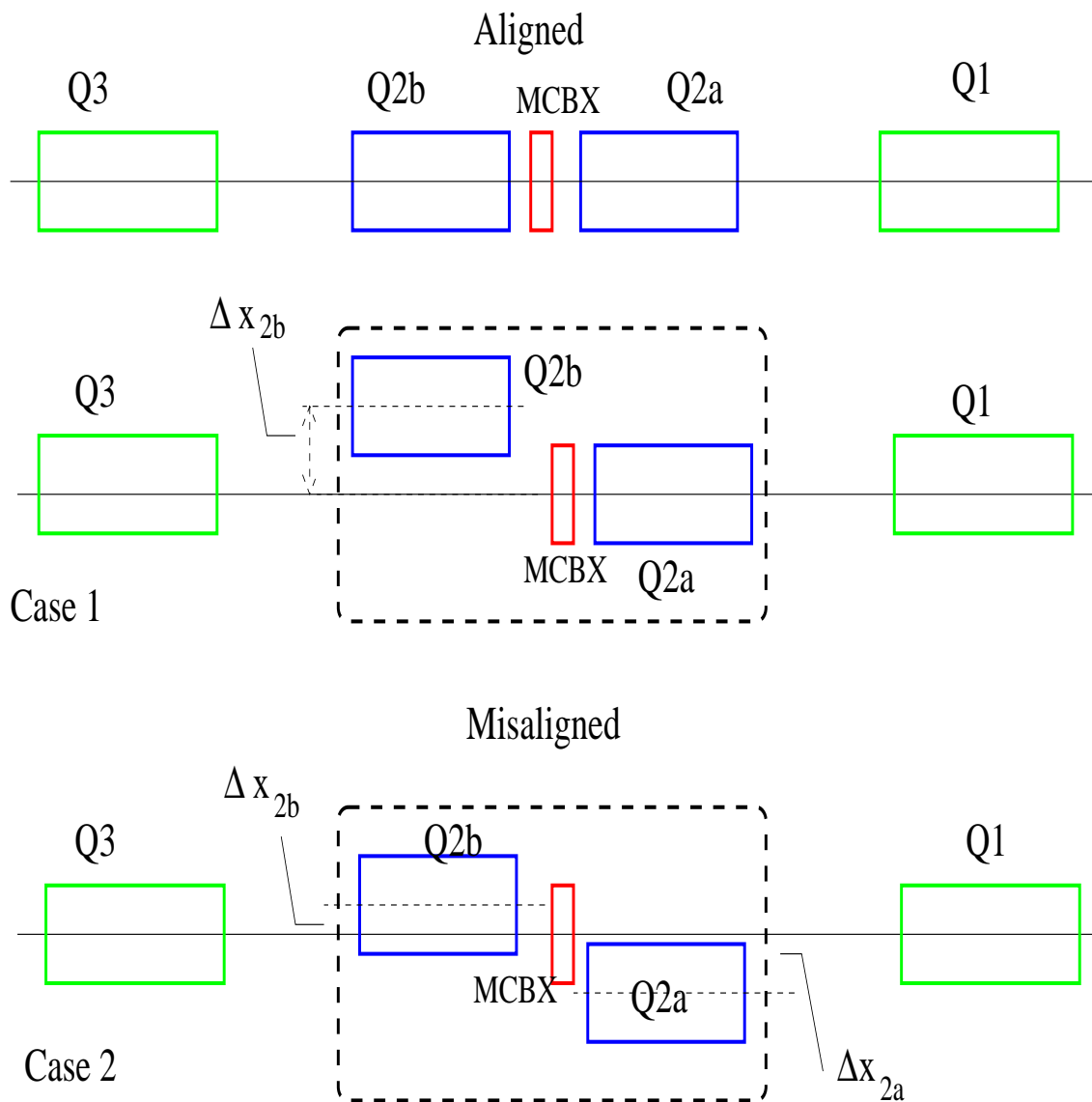
Figure 5: Various alignment positions of the Q2a and Q2b quadrupoles relative to the Q1 and Q3 quadrupoles. In the topmost figure, all quadrupoles are perfectly aligned. The following figures show two possibilities if there is a fixed transverse offset between Q2a and Q2b. For the first misaligned case, the common cryostat containing Q2a and Q2b is centered so that the magnetic center of Q2a is aligned on the common magnetic centers of Q1 and Q3 while Q2b is misaligned. In the second misaligned case, the magnetic centers of both Q2a and Q2b are offset from the common magnetic center. The cryostat is translated rigidly so that the transverse distance between the magnetic centers of Q2a and Q2b is constant.
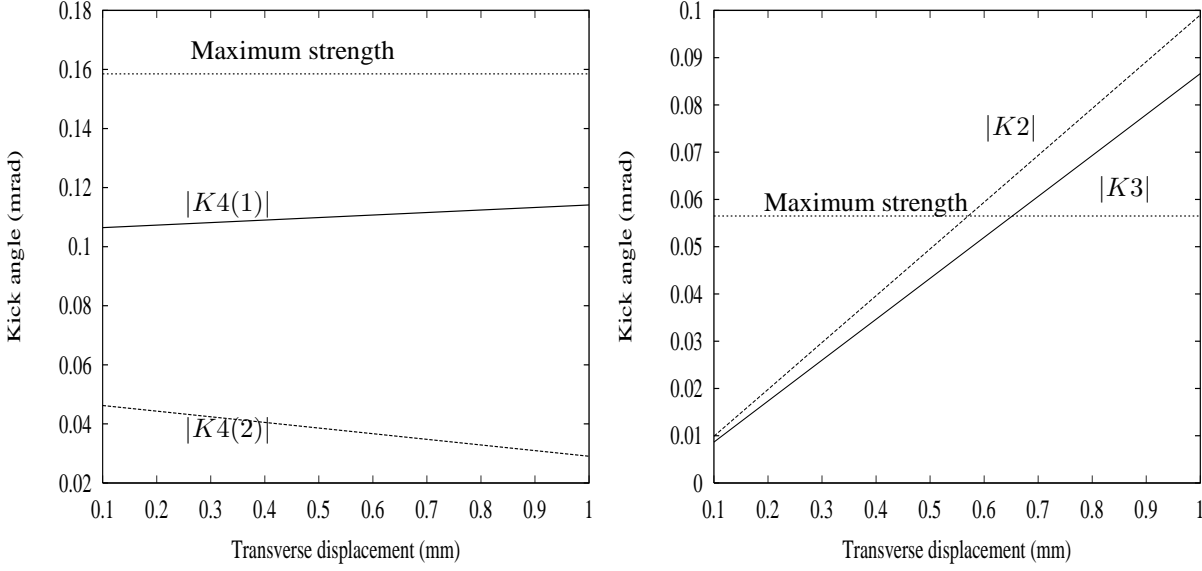
Only Q2b misaligned

Figure 6: Required corrector strengths as a function of the transverse misalignment when only Q2b is misaligned. Left: Absolute strength of K4 vs displacement of Q2b. Right: Absolute strength of MCBX dipole layers vs displacement of Q2b. The strengths of K4 stay well below their maximum strength but the strengths of K2 and K3 reach their upper limits at displacements of 0.55mm and 0.65mm respectively.

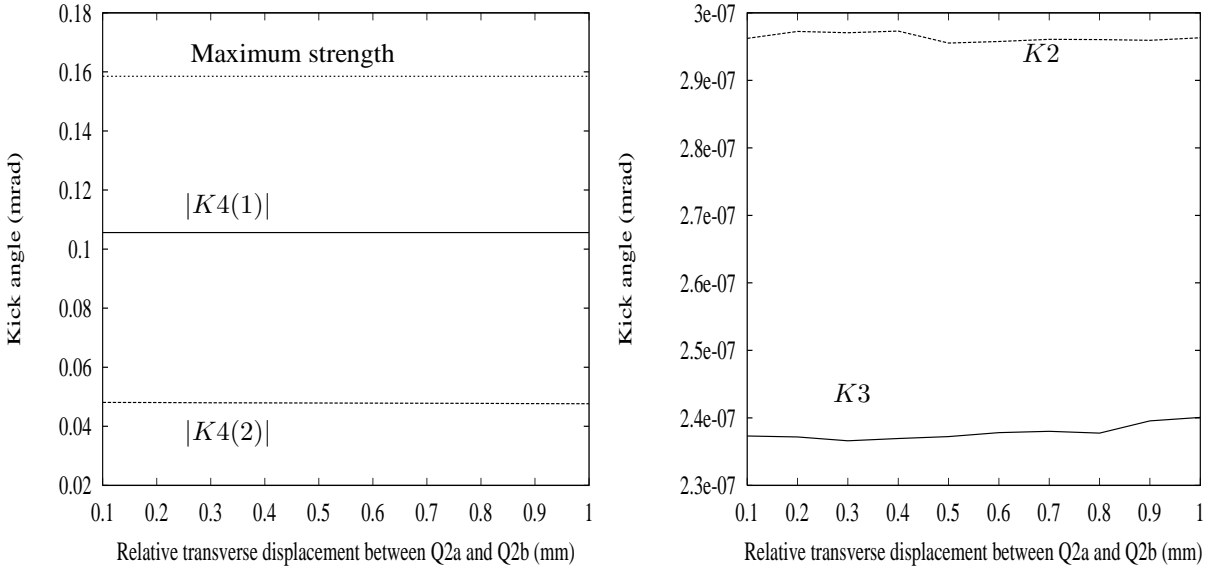**Q2a misaligned to correct for Q2b**

Figure 7: Required corrector strengths as a function of the transverse misalignment when Q2a is appropriately misaligned to correct for the misalignment of Q2b. Left: Absolute strength of K4 vs relative displacement. Right: Absolute strength of MCBX dipole layers vs relative displacement. With this self compensation, the correctors K2 and K3 stay at practically zero strength up to relative displacements of 1mm.
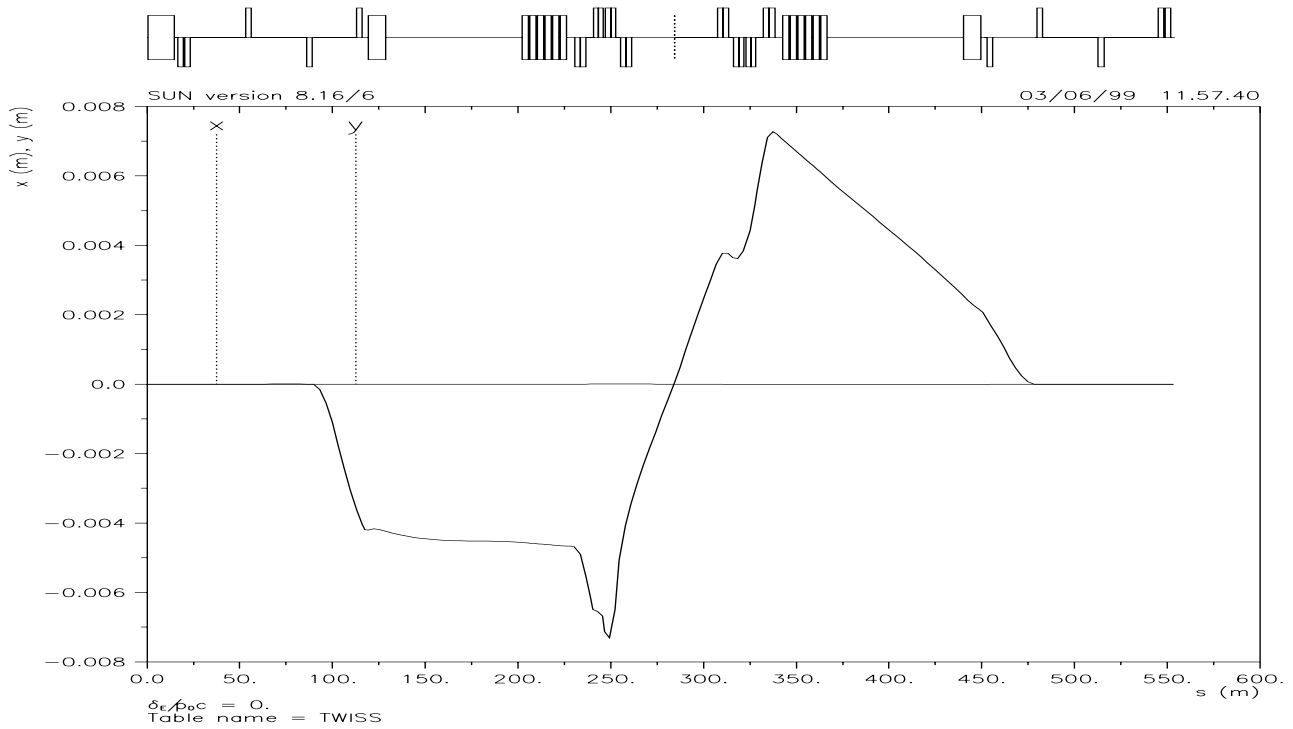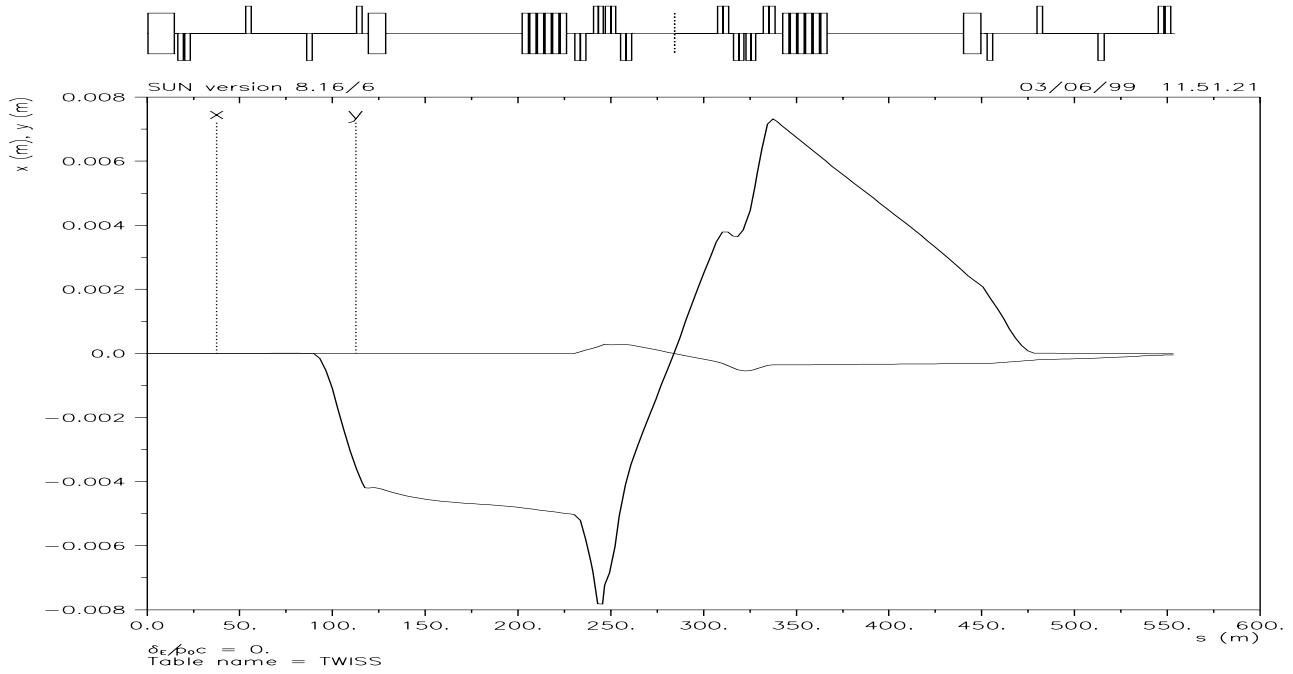
8

Figure 8: Orbit through the IP with horizontal misalignments of Q2a, Q2b upstream of the IP and correction with the dipole correctors in the IR upstream of the IP. Top: Only Q2b is displaced by 0.5mm. The beam is centered at the IP but the orbit correction is not perfect. There is a small crossing angle in the vertical plane and an orbit excursion of about 0.2mm in the downstream quadrupoles. Bottom: A relative misalignment of 1mm between Q2a and Q2b. Both these magnets are misaligned with the common magnetic center to provide compensating kicks. Here the orbit is virtually unchanged from the case without misalignments and the orbit correctors are used only weakly.
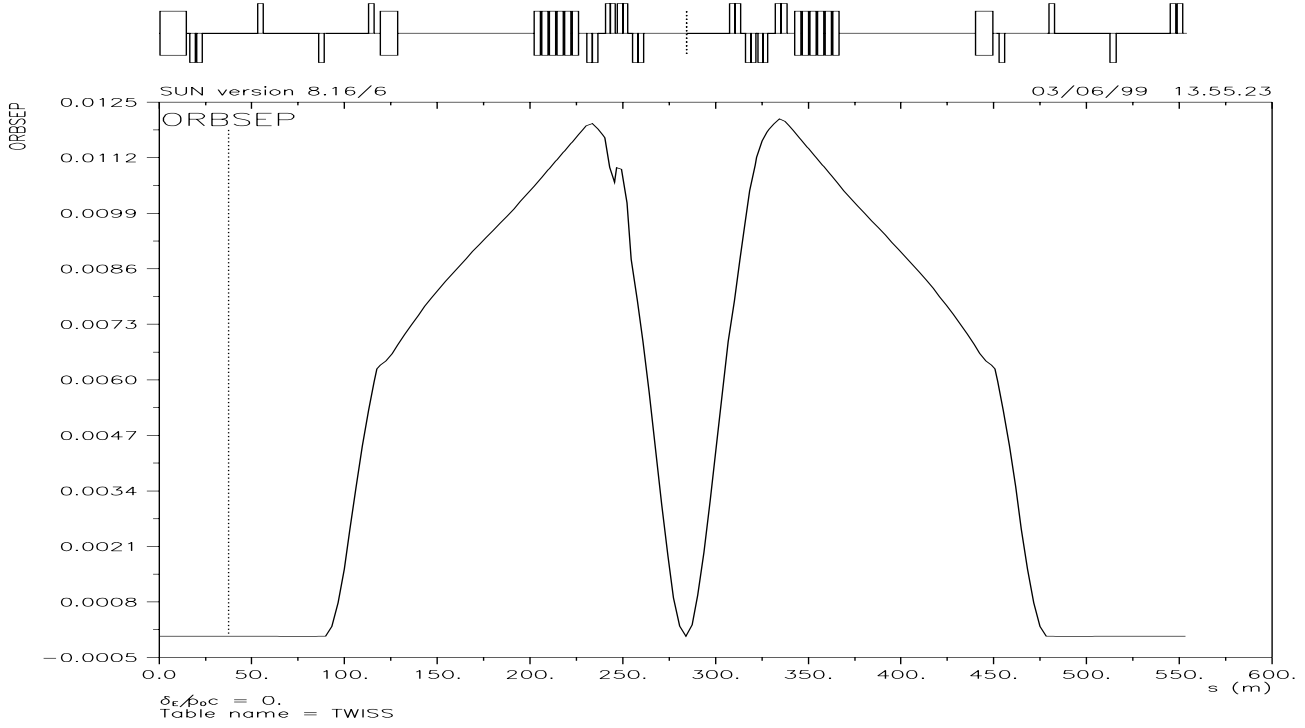
Figure 9: Orbit separation between the beams in the crossing plane when Q2a and Q2b upstream of the IP are both offset from the common axis with a relative misalignment between them of 1mm. The orbit separation between the beams is nearly the same as without any misalignment.
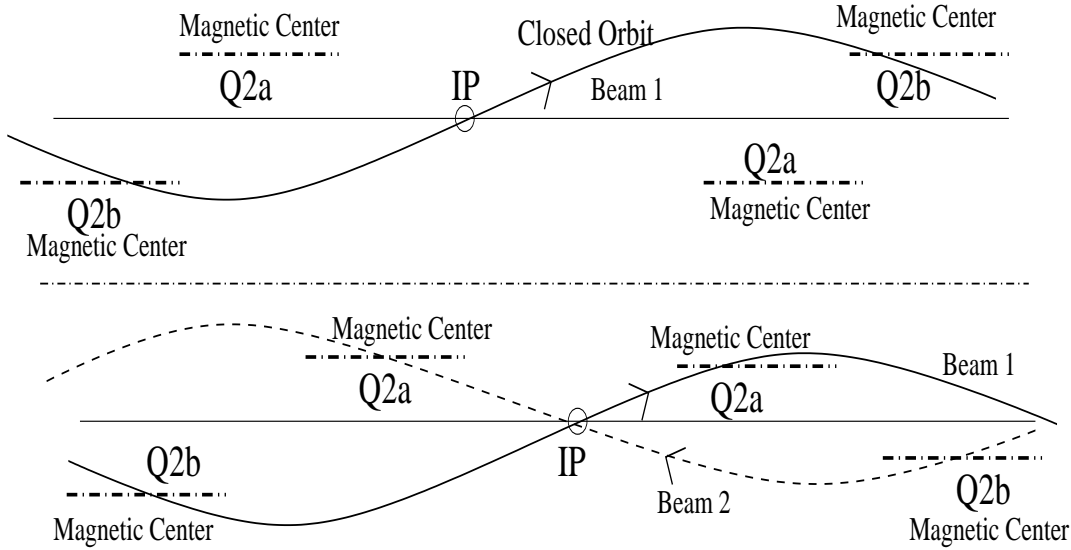
both sides of IP5 are transversely misaligned with their separation fixed at 1mm. Figure 11 shows that with a relative misalignment of this magnitude, the dynamic aperture is not affected significantly for any of the different misalignment settings.

Table 2 shows the dynamic aperture averaged over all 16 angles in coordinate space and over the three seeds. It is evident that there is no significant change in dynamic aperture with relative misalignments of 1mm for any of the three offset settings shown in Figure 10. This is true even for the theoretically worst case (iii) where the tracked beam is further off axis in Q2b on both sides.
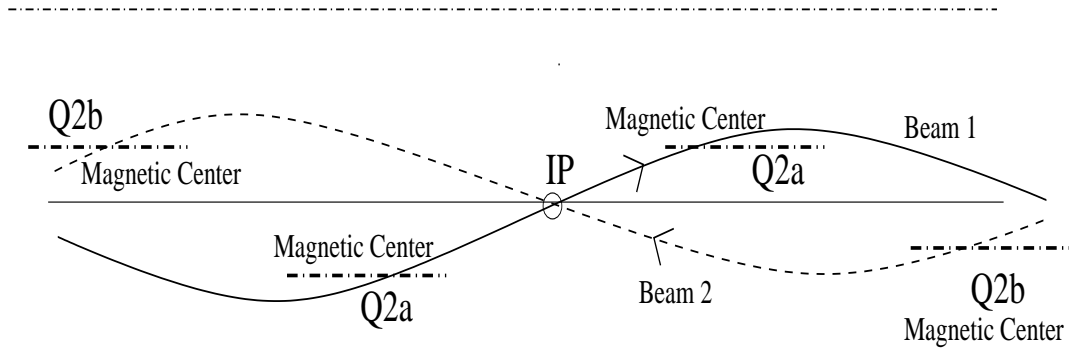
In the calculations of the dynamic aperture of beam 1, we have chosen the ratios of the offsets of Q2a and Q2b to be determined by the beta functions of this beam. The beta functions of beam 2 are different from those of beam 1 at any given location so the orbit of beam 2 will not be exactly compensated. In practice, the ratios of the offsets should be determined so that the orbits of both beams are compensated with minimal use of the orbit correctors. This can be done independent of the size of the relative misalignment between the two pairs of Q2a/Q2b quadrupoles, provided it is of the order of a mm or less. In a possible extreme scenario, one might imagine that there is an offset between the quadrupoles say on the left but none on the right [5]. In this case, beam 1 benefits when Q2b on the left is moved in the direction of the closed orbit of beam 1. One might speculate that the dynamic aperture of beam 2 would suffer because it sees worse fields in Q2b on the left but not compensating better fields in Q2b on the right. However case (iv) in Figure 11 shows that even when a beam sees larger nonlinear fields in Q2b on both sides, the dynamic aperture is not affected. So the compensation of a larger nonlinearity in Q2b with a smaller nonlinearity in Q2a on one side of the IP appears sufficient to preserve the dynamic aperture. The calculations in this section demonstrate that relative offsets of up to 1mm can be successfully compensated without much use of the correctors and with little or no impact on the luminosity or beam stability.

A remaining question is that of a possible impact on the physical aperture [5]. The results in Appendix B show that again with a relative offset of 1mm, the maximum loss in physical aperture is 0.4σ which is less than the 1σ loss that is considered tolerable [1].

10

OPTIMUM OFFSET SETTINGS FOR BEAM 1

Magnetic Center

Closed Orbit

Magnetic Center

Q2a

IP

Beam 1

Q2b

Q2a

Magnetic Center

Q2b

Magnetic Center

Magnetic Center

Magnetic Center

Q2a

Beam 1

Q2a

Q2b

IP

Q2b

Beam 2

Magnetic Center

Magnetic Center

OPTIMUM OFFSETS FOR BOTH BEAMS

Q2b

Magnetic Center

Beam 1

Magnetic Center

IP

Q2a

Magnetic Center

Q2a

Beam 2

Q2b

Magnetic Center

WORST OFFSET SETTINGS FOR BEAM 1

Figure 10: The signs of the alignments of Q2a and Q2b can be chosen to minimize the impact on either one beam or both beams. In order to minimize the impact of the alignment error on a given beam, the magnetic center of Q2b (where the beam is bigger) can be moved in the direction of the closed orbit of this beam. This is shown in the top part of the figure. However it would be more desirable to minimize the impact of the misalignments on both beams. This would require that Q2b be moved in the direction of the closed orbit of the incoming beam as shown in the middle sketch. The bottom sketch shows the worst settings for beam 1 where Q2b is moved away from the closed orbit on both sides. Note that the closed orbits shown here are only schematic and in fact are not symmetric about the IP. Since the signs of the offsets between Q2 and Q2b, once enclosed in the common cryostat, may be random, the optimum offset positioning may be used as a criterion for sorting these quadrupoles.
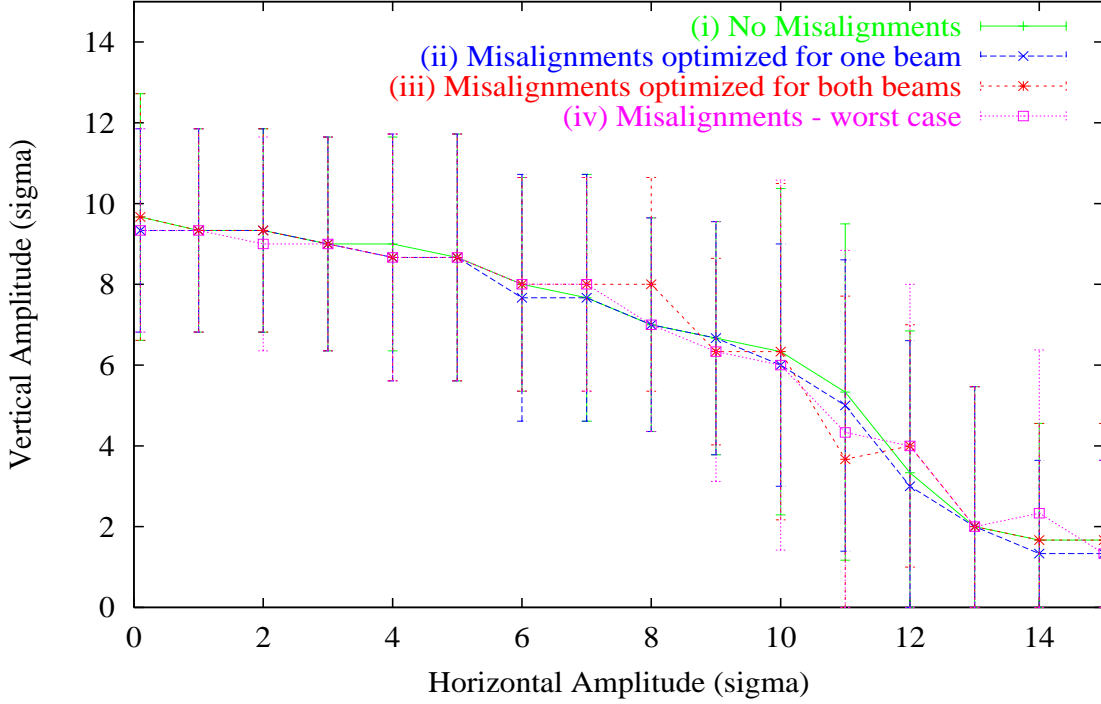
Figure 11: Dynamic aperture when the relative transverse misalignment between Q2a and Q2b is 1mm. Both pairs of quadrupoles, upstream and downstream of the IP, are misaligned. The four cases shown correspond to: (i) no misalignments, (ii) the sign of the misalignments are chosen to reduce the closed orbit offsets for the beam that is tracked, (iii) misalignments are chosen to be neutral for both beams, (iv) misalignments are chosen to increase the closed orbit offsets for the beam that is tracked. In each case, the dynamic aperture is averaged over three seeds. This figure shows that in all cases, the relative misalignment of 1mm does not affect the dynamic aperture significantly.

Relative offset: Δx [mm]	Average Dynamic aperture $\langle DA \rangle \pm \sigma_{\langle DA \rangle}$
None	11.2 ± 1.8
1.0, case (1)	11.1 ± 1.8
1.0, case (2)	11.2 ± 1.8
1.0, case (3)	11.1 ± 1.8

Table 2: The average dynamic aperture calculated over 3 random seeds and 16 angles in coordinate space with and without transverse misalignments. The cases correspond to the three possible misalignment settings shown from top to bottom in Figure 10.
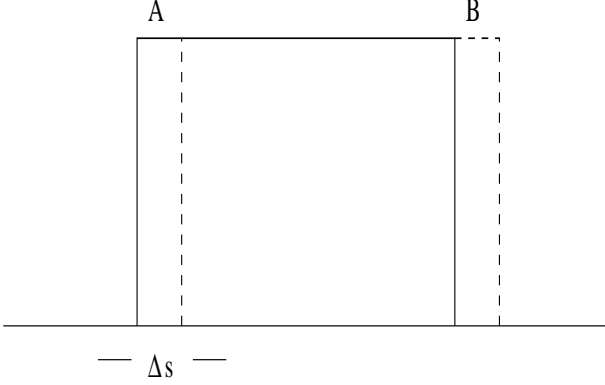
12

3 Longitudinal displacement errors

Figure 12: Longitudinal displacement of a quadrupole by Δs.
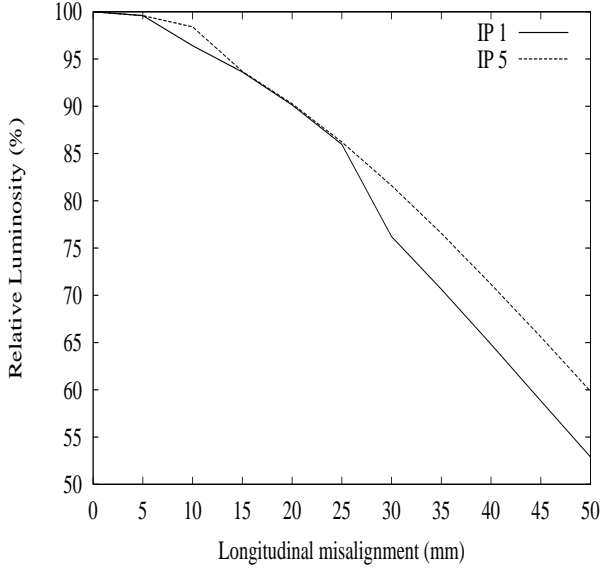

Figure 13: Relative luminosity due to a longitudinal misalignment of Q2b. No orbit corrections. With displacements up to 5mm, the loss of luminosity is less than 1%.

A longitudinal displacement of a quadrupole leads in effect to a gradient error at the locations shown as A and B in Figure 12. Gradient errors lead to tune shifts, β beats and dispersion beats. In addition, when the closed orbit is off-axis through the quadrupole due to the crossing angle, there are also dipole errors leading to closed orbit shifts and consequent loss in luminosity. The magnitudes of these shifts depend on the differences of the beta functions at the ends of the quadrupole.

Figure 13 shows that longitudinal displacements of Q2b by less than 5mm reduce the luminosity by less than 1%. This tolerance on the longitudinal placement is achievable.

The longitudinal displacement error has other effects mentioned above. We find [6] that the tune shifts, maximum beta beat and maximum dispersion beat due to a longitudinal error of a triplet quadrupole (over the length of which the phase advance remains nearly constant) are given by

$$\Delta \nu = \frac{1}{4\pi}(\beta_B - \beta_A)\frac{B'\Delta s}{(B\rho)} \tag{14}$$

$$\left(\frac{\Delta\beta}{\beta}\right)_{max} = \frac{1}{2\sin 2\pi\nu}(\beta_B - \beta_A)\frac{B'\Delta s}{(B\rho)} \tag{15}$$

$$\Delta D_{max} = \frac{\sqrt{\beta_{max}}}{2\sin\pi\nu}(\sqrt{\beta_B}D_B - \sqrt{\beta_A}D_A)\frac{B'\Delta s}{(B\rho)} \tag{16}$$

Table 3 shows the changes in these quantities due to a misalignment error of 1mm in each of the triplet quadrupoles. These changes are negligibly small, and in fact can be easily corrected with usual linear corrections if desired, so we conclude that longitudinal displacement errors of 1mm will have little impact on the beam.

Quadrupole	$(\Delta\nu_x, \Delta\nu_y)$	$[(\Delta\beta_x/\beta_x)_{max}, (\Delta\beta_y/\beta_y)_{max}]$	$\Delta D_{x.max}$ [mm]
Q1	(0.14E-06, 0.83E-06)	(0.95E-06, 0.57E-05)	0.25
Q2a	(0.87E-07, 0.97E-06)	(0.58E-06, 0.67E-05)	0.30
Q2b	(0.68E-06, -0.53E-06)	(0.46E-05, -0.37E-05)	0.38
Q3	(0.77E-06, -0.55E-06)	(0.52E-05, -0.38E-05)	1.6

Table 3: Changes in the tunes, beta functions and horizontal dispersion due to a longitudinal displacement error of 1mm in each of the triplet quadrupoles.
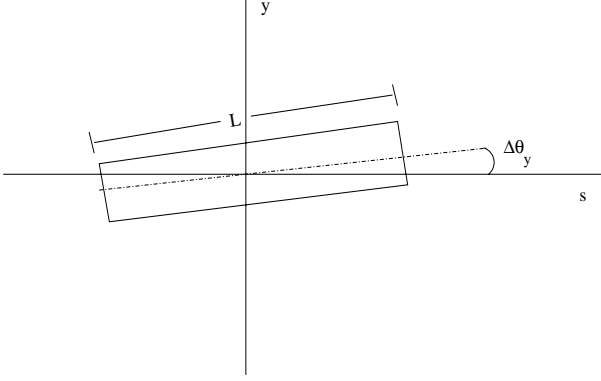
4 Rotational misalignments

Figure 14: Quadrupole rotated about a transverse axis at its longitudinal center.

Suppose a quadrupole is rotated about the x axis in the (y, s) plane by a small angle $\Delta\theta_y$. We assume for now that the quadrupole is rotated about its longitudinal center as shown in Figure 14. Due to the rotational misalignment, a particle on the closed orbit is offset from the magnetic center of the quadrupole by an amount $\Delta y \approx s\Delta\theta_y$ for $\Delta\theta_y \ll 1$, s is the longitudinal distance from the longitudinal center of the quadrupole. If B' is the gradient in the quadrupole, the field along the x axis is changed to

$$B_x = B'(y + \Delta y) \simeq B'y + B's\Delta\theta_y \qquad (17)$$

A dipole field is created with a sign depending on the sign of the offset of the particle orbit from the magnetic center of the quadrupole. This leads to a closed orbit shift in the vertical plane and will also lead to a change in the tune when nonlinear elements are present. The phase advance along the length of a triplet quadrupole changes very little so the closed orbit distortion at any point in the ring is

$$y(s) = \frac{\sqrt{\beta_y(s)}}{2\sin\pi\nu_y} \frac{B'\Delta\theta_y}{(B\rho)} \cos[\pi\nu_y - |\mu_y(s) - \mu_y(Q)|] \int_{-L/2}^{L/2} \sqrt{\beta_y(s')} s' ds' \qquad (18)$$

where L is the total length of the quadrupole and $\mu_y(Q)$ is the phase advance at the location of the quadrupole. If β_y were symmetric about the longitudinal center of the quadrupole, then the effects of the dipolar kicks would be cancelled between the two halves of the quadrupole and there would be no closed orbit shift. This is not the case for the beta functions within the triplets as can be seen in Figure A.1 in Appendix A. The IP is at a phase advance of $\pi/2$ from nearly each of the triplet quadrupoles so the orbit shift at the IP is

$$y_{IP} = \frac{\sqrt{\beta_y^*}}{2} \frac{B'\Delta\theta_y}{(B\rho)} \int_{-L/2}^{L/2} \sqrt{\beta_y(s')} s' ds' = \frac{\sqrt{\beta_y^*}}{2F} \frac{\Delta\theta_y}{L} \int_{-L/2}^{L/2} \sqrt{\beta_y(s')} s' ds' \qquad (19)$$

If the quadrupole were to be rotated at a distance d from its longitudinal center, the above expression would be replaced by

$$y_{IP} = \frac{\sqrt{\beta_y^*}}{2F} \frac{\Delta\theta_y}{L} \int_{-L/2}^{L/2} \sqrt{\beta_y(s')} (s' - d) ds' \qquad (20)$$

This orbit shift at the IP would lead to a loss in luminosity.

Figure 15 shows that if uncorrected, a pitch or yaw of more than 1μrad will be sufficient to cause an observable loss in luminosity. This degree of angular alignment would require that over the 5.5m length of each Q2a, Q2b, the two quadrupoles have to be aligned within $5.5 \times 1.0/2 = 2.75 \mu$m of each other. This high degree of precision is unrealistic so orbit correction will be required.

Figure 16 shows two possible ways of aligning the Q2a/Q2b assembly in the tunnel. The top part of the figure shows the first possibility where Q2a is aligned with the common magnetic center of Q1 and Q3. In this case, all of the orbit correction has to be done with the dipole correctors. The bottom part of the figure shows another possibility where the common cryostat is rotated so that both Q2a and Q2b are misaligned with other quadrupoles but in such a way that the effect on the orbit is minimal. In this case, due to the compensating kicks from these quadrupoles, the beams are still centered at the IP and the required strength of the orbit correctors is weak.

4.1 Pitch

Here we will consider the case where a single Q2b is misaligned with respect to the Q2a in the common cryostat. First we will examine the orbit correction that is necessary and then the maximum allowable pitch angle that preserves the dynamic aperture.
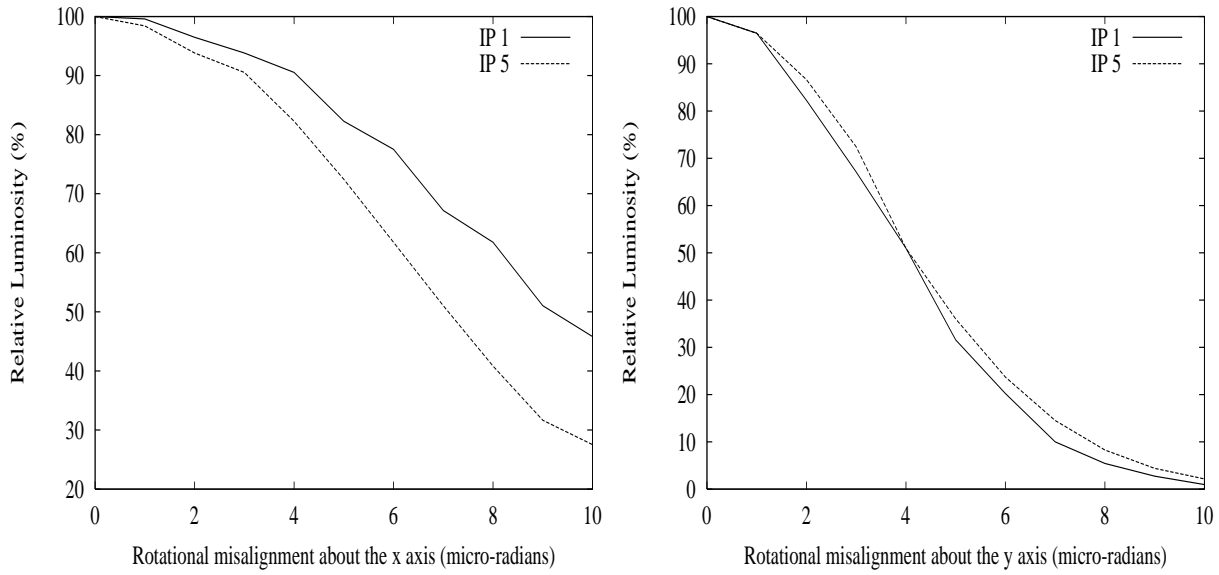
Figure 15: Relative luminosity due to a rotational misalignment of a single Q2b upstream of the IP in IR5 about the horizontal axis or pitch (left) and the vertical axis or yaw (right). No orbit corrections in either case.

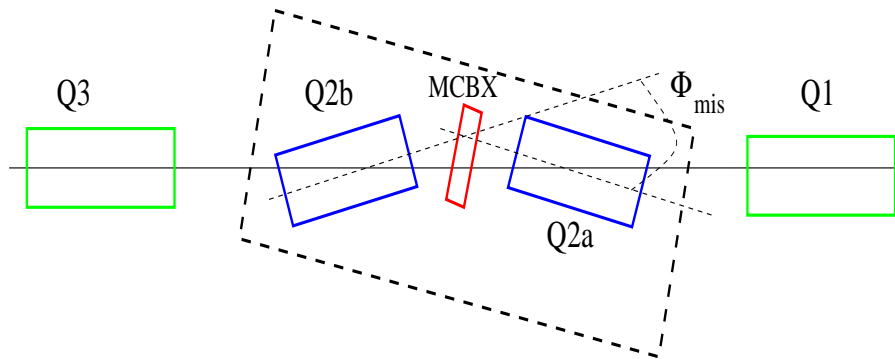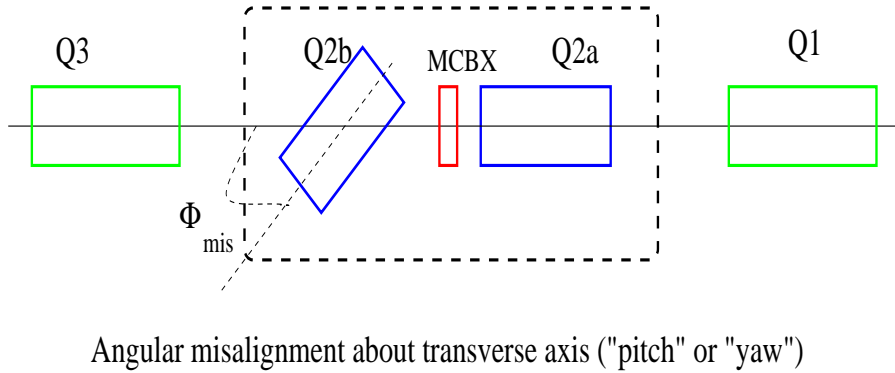Angular misalignment about transverse axis ("pitch" or "yaw")

Figure 16: Two possible orientations when there is a relative misalignment between Q2a and Q2b. In the top figure, Q2a is aligned with the common magnetic axis while in the bottom figure, the misalignment with respect to the common axis is split between the two quadrupoles. In the latter case, the orbital effects of the misalignments are self-compensating.
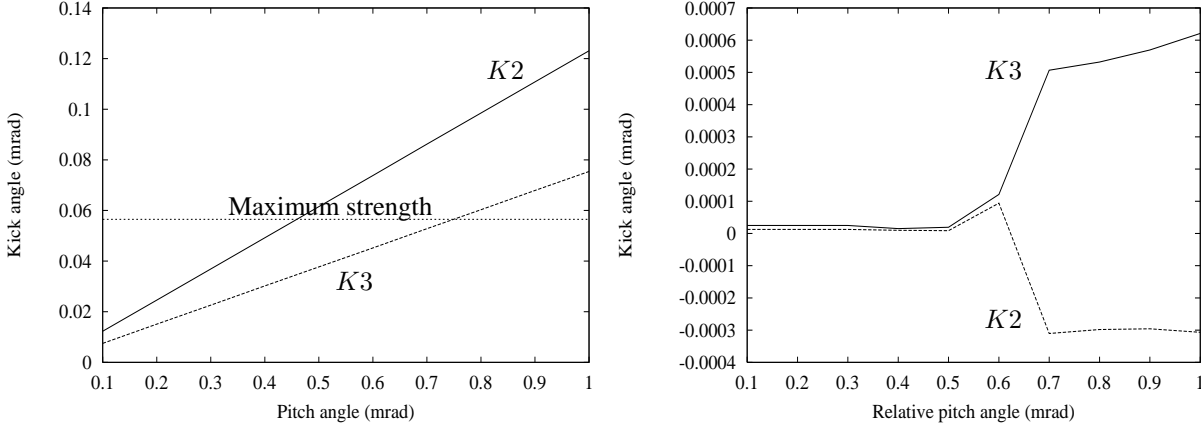
Figure 17: Absolute strength of MCBX dipoles as a function of the relative pitch angle. Left: Only Q2b is misaligned. The maximum corrector strength is reached at a pitch angle of about 0.45mrad. Right: Q2a is appropriately misaligned to correct for the misalignment of Q2b. Over this range of pitch angles, the corrector strengths are two orders of magnitude below their maximum strength.

	$|K4(1)|$ [mrad]	$|K4(2)|$ [mrad]	$|K2|$ [mrad]	$|K3|$ [mrad]
No multipole errors	0.106	6.69×10^{-3}	3.07×10^{-4}	6.21×10^{-4}
Average over 5 seeds	0.106	6.58×10^{-3}	4.37×10^{-4}	7.17×10^{-4}

Table 4: Corrector strengths required to correct a relative pitch angle of 1mrad. The first row shows the strengths without multipole errors in the IR quadrupoles, the second row shows the strengths averaged over 5 random errors. Maximum strength of the $K2$ and $K3$ dipoles is about 0.056mrad while the maximum strength of $K4$ dipoles is 0.158mrad. This table shows that with self-compensating pitch misalignments, only weak corrector strengths are required.

A pitch misalignment distorts the vertical orbit. We correct for the orbits of both beams using the same correctors as used for transverse misalignments in Section 2.2. Figure 17 shows the required strengths of the MCBX correctors as a function of the pitch angle when only Q2b is misaligned. The maximum pitch angle that can be corrected is about 0.45mrad before the strength of K2 exceeds the available strength. Figure 17 also shows the required strengths when Q2a is misaligned to compensate the effect on the orbit due to the misalignment of Q2b. In both cases, the crossing angle dipoles K4 are used at about their nominal strengths. Since the orbit distortion is $\propto \sqrt{\beta}$, we expect that $\Delta\phi(Q2a)/\Delta\phi(Q2b) = -\sqrt{\beta(Q2b)/\beta(Q2a)}$ where the pitch angles $\Delta\phi$ are measured with respect to the common magnetic center of the other quadrupoles. Using MAD, we find that the effect on the orbit is minimized when the pitch angles satisfy $\Delta\phi(Q2a) = -1.1\Delta\phi(Q2b)$, close to what we expect. The relative pitch angle between Q2a and Q2b is $|\Delta\phi(Q2a)| + |\Delta\phi(Q2b)|$. With this setting, figure 17 shows that the correctors are used very weakly and even up to a total relative pitch angle of 1mrad, the strengths are about two orders of magnitude below the maximum strengths.

We have corrected the orbit in the absence of multipole errors in the IR quadrupoles. However when these multipole errors are included, the particles are subject to additional orbit kicks and the corrector strengths change. We have calculated the strengths required to correct a relative pitch angle of 1mrad for five different seeds of these error fields. Table 4 shows that even with the errors, the corrector strengths do not change significantly and even at a total relative pitch angle of 1mrad, the strengths are about two orders of magnitude below the maximum value.
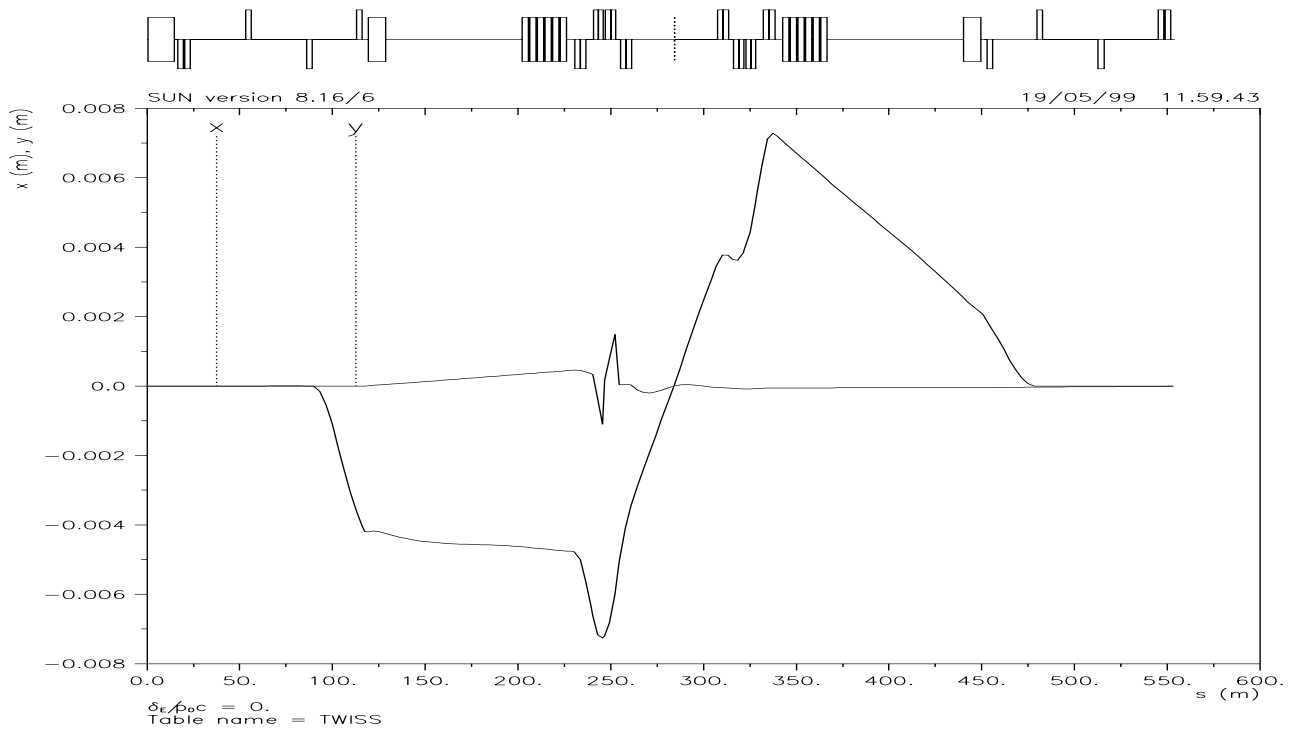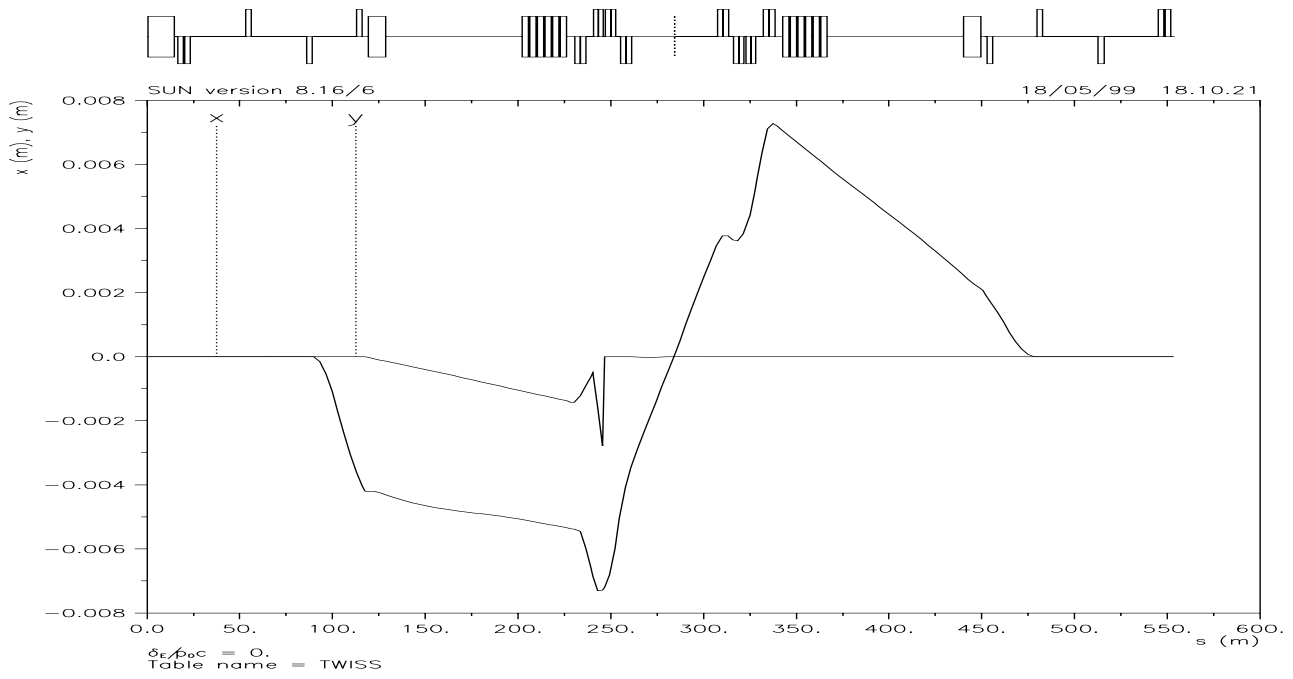
Figure 18: Orbit through the IR with pitch misalignments upstream of the IP. Top: Only Q2b has a pitch misalignment of 0.5mrad. Bottom: A relative pitch angle of 0.5mrad between Q2a and Q2b.
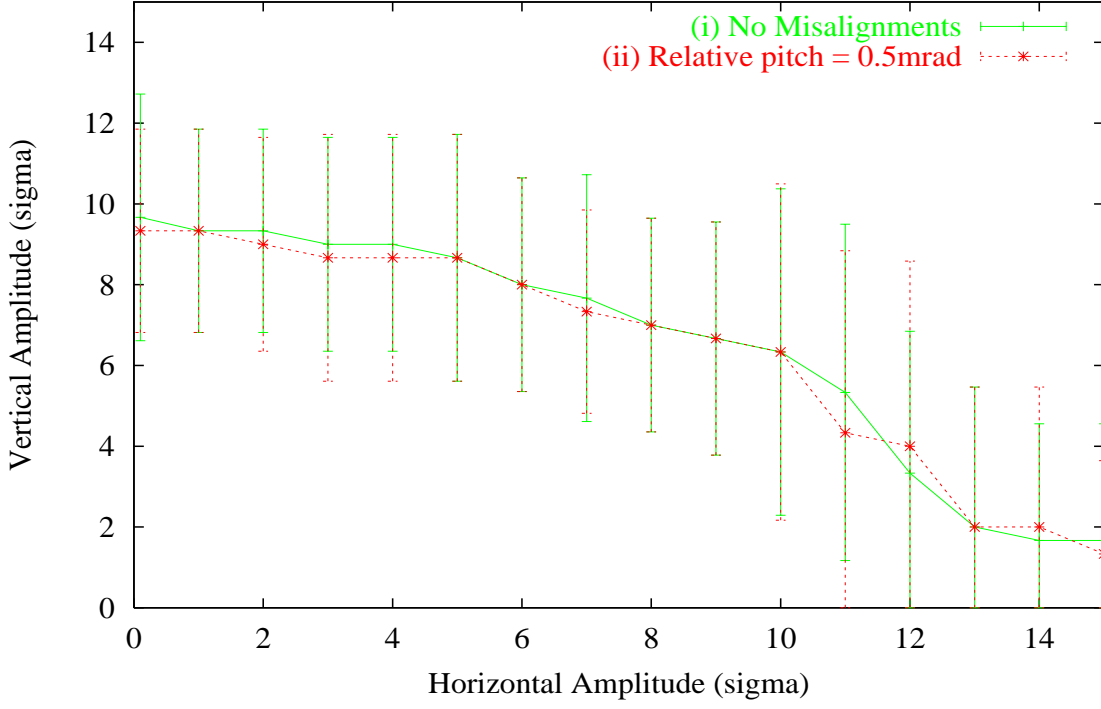
Figure 20: Dynamic aperture when the relative pitch misalignment between Q2a and Q2b is 0.5mrad. The two cases shown correspond to: (i) no misalignments, (ii) the relative pitch angle between Q2a and Q2b is 0.5mrad. This figure shows that the relative misalignment of 0.5mrad does not affect the dynamic aperture significantly.

Relative pitch: $\Delta\phi$ [mrad]	Average Dynamic aperture $\langle DA \rangle \pm \sigma_{\langle DA \rangle}$
None	11.2 ± 1.8
0.5	11.1 ± 1.9

Table 5: The average dynamic aperture calculated over 3 random seeds and 16 angles in coordinate space with and without pitch misalignments.
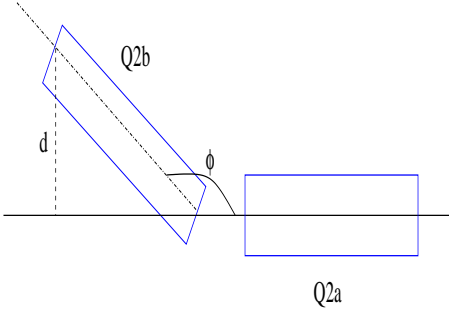
Figure 19: The transverse distance d between the end of Q2a and the far end of Q2b when there is a rotational misalignment between the two quadrupoles.

The rotational misalignment between the two quadrupoles will be determined by the precision with which the ends of the quadrupoles can be aligned. The transverse distance between the ends, $d = l\tan\phi$ is equal to 2.75mm assuming a magnetic length of 5.5m and a rotational angle of 0.5mrad. The ends of the magnets can be aligned to better than this distance so we will limit ourselves to rotational misalignments of up to 0.5mrad.

The dynamic aperture is calculated as earlier by tracking particles over 15 angles in configuration space over 1024 turns with aperture restrictions at ± 30mm. Three random seeds are used for the multipole errors. Figure 20 shows that the dynamic aperture at all angles is not significantly affected by a relative pitch misalignment of 0.5mrad. Table 5 shows that the dynamic aperture averaged over all angles with the pitch misalignment is nearly the same as without.

18

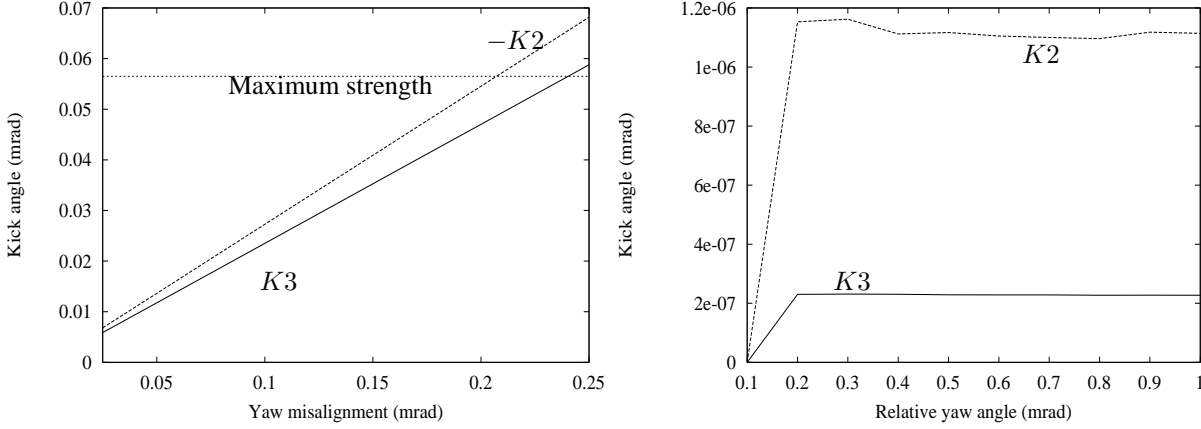Figure 21: Absolute strength of MCBX dipoles vs relative yaw angle. Left: Only Q2b is misaligned. The maximum corrector strength is reached at a yaw angle of about 0.2mrad. Right: Q2a is appropriately misaligned to correct for the misalignment of Q2b. In this case, corrector strengths are about four orders of magnitude below their maximum strength.

4.2 Yaw

A yaw misalignment (rotation about the vertical axis) distorts the horizontal orbit the most. If there is a crossing angle in the horizontal plane (as is the case at IR5), then this increases the maximum closed orbit excursion in the triplets beyond 7.5mm. Figure 21 shows that the maximum yaw angle that can be corrected is about 0.2mrad if only Q2b is misaligned. A compensating misalignment of Q2a can be used to correct for most of the orbit distortion. The required misalignment $\Delta\theta \propto 1/\sqrt{\beta}$ so $\Delta\theta(Q2a)/\Delta\theta(Q2b) \simeq -\sqrt{\beta(Q2b)/\beta(Q2a)}$ with the total relative misalignment equal to $|\Delta\theta(Q2a)| + |\Delta\theta(Q2b)|$. We find, using MAD, that the orbit distortion is minimized when $\Delta\theta(Q2a) = -1.08\Delta\theta(Q2b)$. Figure 21 also shows that with these self-compensating misalignments, correctors are needed at very weak strengths even up to misalignments of 1mrad. Again, in both cases the crossing angle dipoles K4 are used at close to their nominal values.

	$|K4(1)|$ [mrad]	$|K4(2)|$ [mrad]	$|K2|$ [mrad]	$|K3|$ [mrad]
No multipole errors	0.104	2.80×10^{-6}	1.11×10^{-6}	2.27×10^{-7}
Average over 5 seeds	0.103	5.42×10^{-5}	1.86×10^{-4}	9.57×10^{-5}

Table 6: Corrector strengths required to correct a relative yaw angle of 1mrad. The first row shows the strengths without multipole errors in the IR quadrupoles, the second row shows the strengths averaged over 5 random errors. Maximum strength of the $K2$ and $K3$ dipoles is about 0.056mrad while the maximum strength of $K4$ dipoles is 0.158mrad. This table shows that with self-compensating yaw misalignments, only weak corrector strengths are required.

Table 6 shows that even when multipole errors are included, the required corrector strengths are still very weak with a relative yaw misalignment of 1mrad.

Figure 23 and Table 7 confirm that a relative yaw misalignment of 0.5mrad does not affect the dynamic aperture significantly.
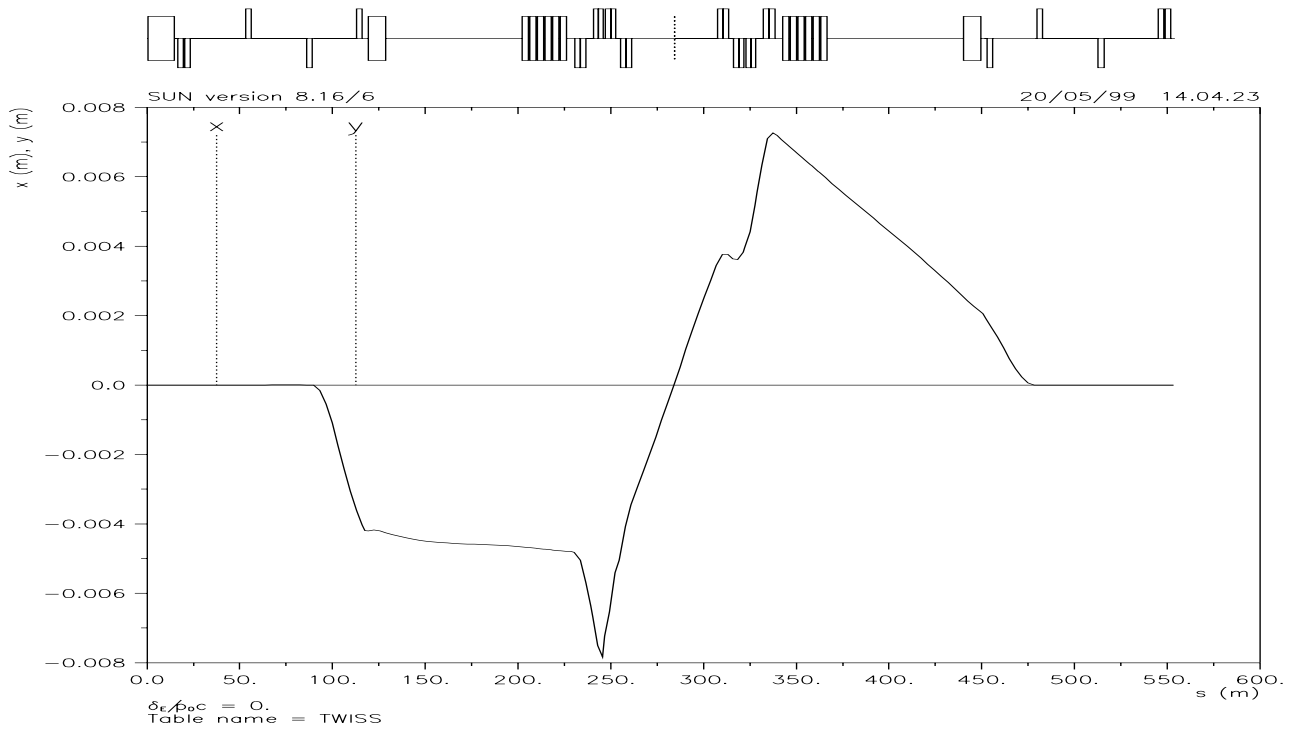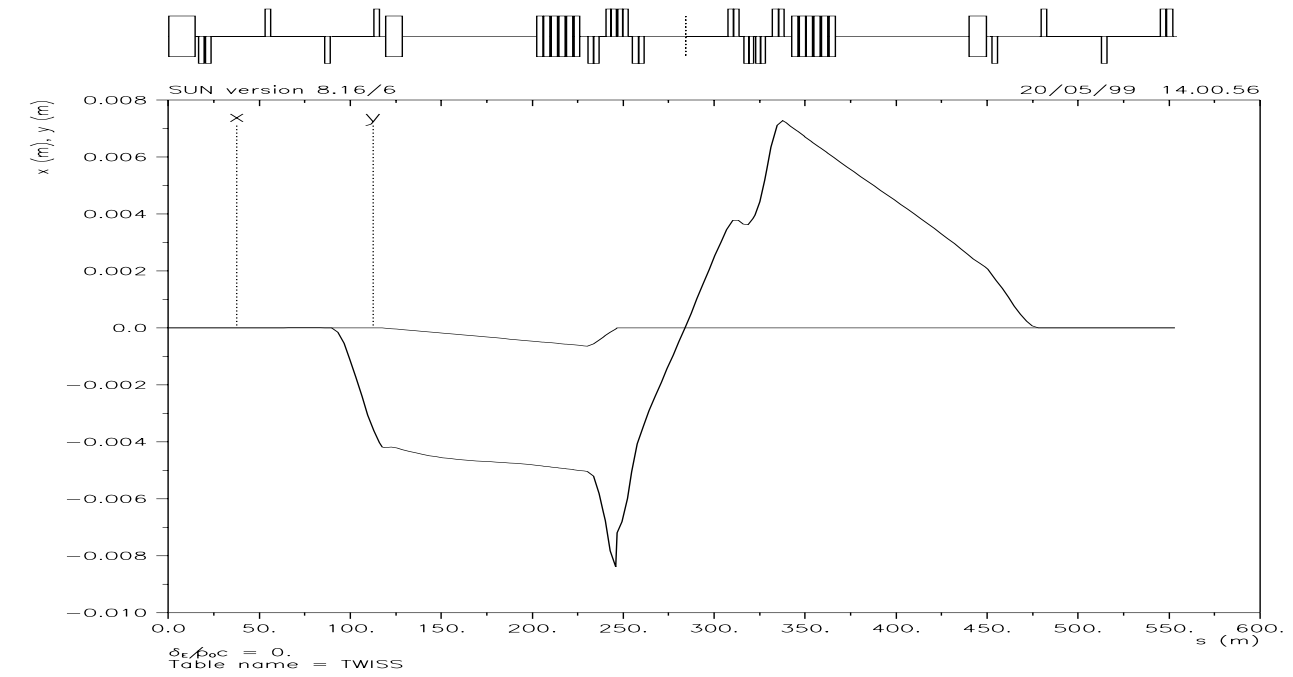
Figure 22: Orbit through the IP with yaw misalignments. Top: Only Q2b has a yaw misalignment of 0.2mrad. This is the maximum possible angle before the corrector strengths are saturated as seen in Figure 21. The orbit is corrected at the IP and at the ends but there is an orbit excursion of about 0.5mm in the quadrupoles. Bottom: A relative yaw angle of 0.2mrad between Q2a and Q2b. Here the orbit is virtually the same as without any misalignments.
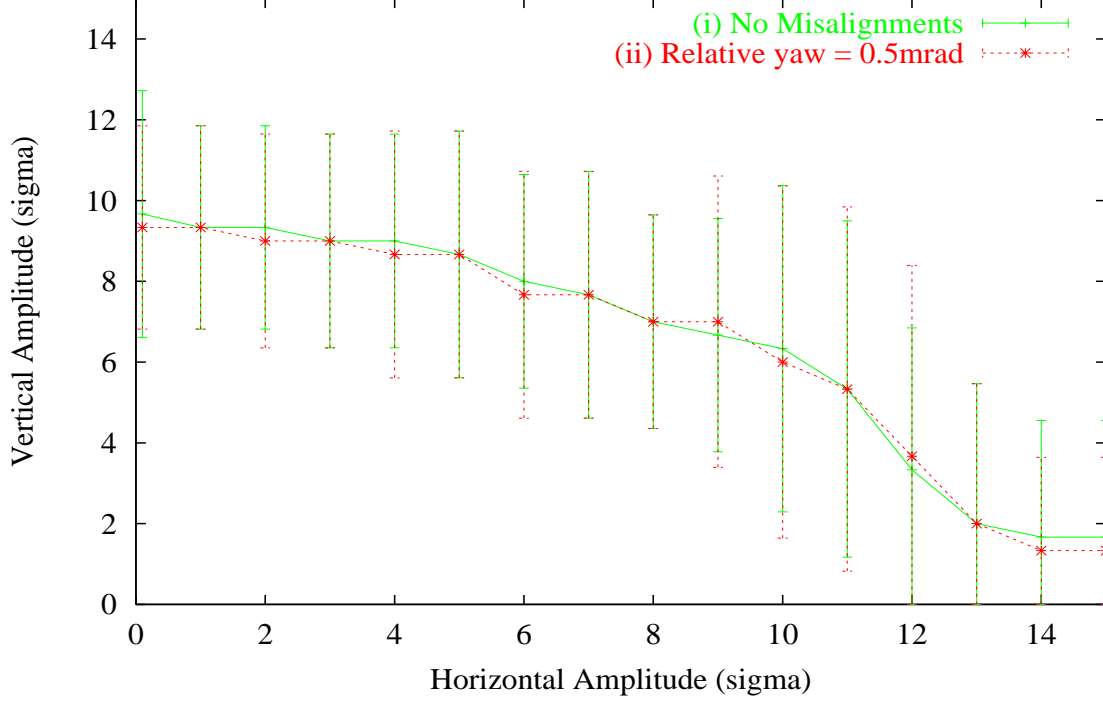
Figure 23: Dynamic aperture when the relative yaw misalignment between Q2a and Q2b is 0.5mrad. Particles are tracked for 1024 turns, three random seeds are used for the multipole errors. The two cases shown correspond to: (i) no misalignments, (ii) the relative yaw angle between Q2a and Q2b is 1mrad. This figure shows that the relative misalignment of 0.5mrad does not affect the dynamic aperture significantly.

Relative yaw: $\Delta\theta$ [mrad]	Average Dynamic aperture $\langle DA \rangle \pm \sigma_{\langle DA \rangle}$
None	11.2 ± 1.8
0.5	11.1 ± 1.8

Table 7: The average dynamic aperture calculated over 3 random seeds and 16 angles in coordinate space with and without yaw misalignments.

Rolled Quadrupole, $\Delta\psi = 1$mrad	$\Delta\nu^{diff}$	D_y(IP)[mm]
Q1	0.024	-1.1
Q2a	0.033	1.6
Q2b	0.042	2.0
Q3	0.054	-2.6

Table 8: Minimum tune splits and vertical dispersion generated at the IP due to a roll angle of 1mrad in each of the triplet quadrupoles.

4.3 Roll

If a quadrupole is rotated about the longitudinal axis so that the pole faces are rotated from the 45° axes by $\Delta\psi$, the fields due to the rotated quadrupole are

$$B_x = B'(y\cos 2\Delta\psi - x\sin 2\Delta\psi), \quad B_y = B'(x\cos 2\Delta\psi + y\sin 2\Delta\psi) \quad (21)$$

The skew quadrupole field couples the motion between the two planes. This has many undesirable consequences including tune shifts, beating between the horizontal and vertical betatron oscillations, induced vertical dispersion and reduced dynamic aperture. We will address these issues here.

The strength of the coupling is measured by the minimum difference between the two eigentunes. This minimum difference is given by

$$\Delta\nu^{diff} = \frac{\sqrt{\beta_x\beta_y}}{\pi}\frac{B'L_q}{(B\rho)}\Delta\psi \quad (22)$$

It is proportional to square root of the product of the beta functions so rotational misalignments of the triplet quadrupoles will have a significant impact on the coupling in the lattice. Using this expression and the table of beta functions in Table A.1, we find the minimum tune splits shown in Table 8 for a roll angle of 1mrad. This shows that 1mrad roll angle in any of the triplet quadrupoles would give rise to an unacceptably large coupling and would require correction.

It was shown in [7] that the relative difference between the normal mode beta function and the usual beta function, e.g. $[\beta_1 - \beta_x]/\beta_x \propto K_{sk}^2/\sin[\pi(\nu_x + \nu_y)]$ where K_{sk} is the skew quadrupole strength. In this case $K_{sk} \propto \Delta\psi$, so the beta beating depends on $\Delta\psi^2$, a small quantity. Furthermore the nominal LHC tunes (ν_x=63.31, ν_y=59.32) are far from the sum resonance. Hence the beta beating and consequent loss of luminosity should be small for roll angles up to 1mrad.
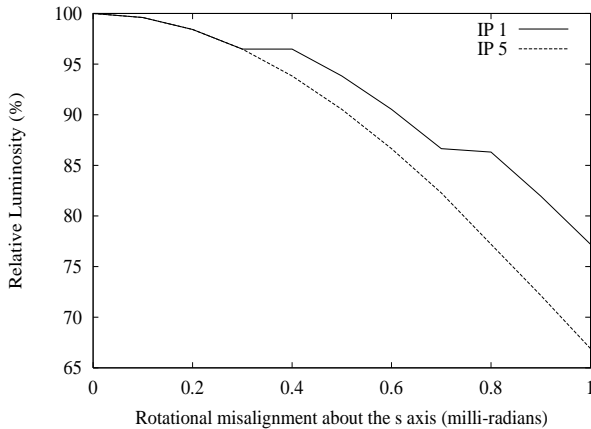
Figure 24: Relative luminosity due to a roll of Q2b without any orbit corrections. The crossing angle combines with the roll to create an orbit shift in the plane orthogonal to the crossing plane.

There is, however, a separate effect which has an impact on the luminosity. Due to the crossing angle, the orbit in the crossing plane goes off-center through these quadrupoles and coupling due to the quadrupole roll introduces an offset in the transverse plane orthogonal to the crossing plane. If not corrected, this orbit offset at the IP will lead to a reduction in the luminosity. This in fact leads to a more stringent tolerance on the allowable roll angle. Figure 24 shows e.g. that a roll angle of 0.2mrad in Q2b is sufficient to reduce the luminosity by nearly 2%. Larger roll angles would require correction.

A rolled quadrupole also generates vertical dispersion if the horizontal dispersion at the quadrupole location is non-zero. To lowest order in $\Delta p/p$, the equation of motion for the vertical dispersion is

$$D_y'' + K_y(s)D_y = \frac{B'}{(B\rho)}2\Delta\psi D_x^0 \quad (23)$$

where B' is the gradient of the rolled quadrupole and D_x^0 is the horizontal dispersion at the quadrupole. The periodic

solution of this equation is

$$D_y(s) = \left\{ \frac{\sqrt{\beta_y(s)\beta_{y,q}}}{\sin \pi \nu_y} \frac{B'L_q}{(B\rho)} \cos[\pi \nu_y - |\psi_y(s) - \psi_y^0|] \right\} D_x^0 \Delta \psi \tag{24}$$

The phase advance from any of the triplet quadrupoles to the IP is nearly $\pi/2$ so the vertical dispersion generated at the IP is

$$D_y(IP) = \left\{ \sqrt{\beta_y(s)\beta_{y,q}} \frac{B'l_q}{(B\rho)} \right\} D_x^0 \Delta \psi \tag{25}$$

The vertical dispersion at the IP is calculated with the values of the beta functions and dispersion given in Appendix A. The values are shown in Table 8. In section 2.1 we showed that a dispersion of 29mm at the IP is required to reduce the luminosity by 2%. The values in this table are one order of magnitude smaller and therefore will have no significant impact on the luminosity. In addition, the dispersion due to the roll angle will most likely be negligible compared to other effects such as the feeddown from skew multipoles.

The orbit shift due to a roll angle can be corrected by the use of the dipole correctors in the IR. Figure 25 shows that orbit shifts due to a roll angle in Q2b of up to 1mrad can be compensated with these correctors with only minimal use of the dipole correctors. The orbit shift therefore does not impose a realistic limit on the allowable roll.

Effects due to coupling require the use of the skew quadrupole correctors in the MCQS packages. The strength of the difference coupling resonance $\nu_x - \nu_y = p$ is given by the complex coefficient

$$C_{diff} = \frac{1}{2\pi} \oint \sqrt{\beta_x \beta_y} K_{sk} \exp[i(\psi_x - \psi_y - (\nu_x - \nu_y - p)\frac{s}{R})]ds \tag{26}$$

where K_{sk} is the strength of the skew quadrupole at location s. The decoupling criterion we will use is to set the contribution to C_{diff} from the triplets on both sides of an IP to zero. This is a local decoupling criterion which may be different from the decoupling scheme (whether local or global) to be used in the LHC. Skew quadrupoles can also excite the linear sum coupling resonance $\nu_x + \nu_y = p$ but at the nominal LHC V5.1 tunes (ν_x=63.31, ν_y=59.32) we may assume that the tunes in all accesible regions of phase space will be far from the sum resonance even after the skew quadrupoles in the IR are turned on. Defining the real and imaginary parts of this difference resonance phasor

$$\mathcal{R} = 2\sum_i^8 (\sqrt{\beta_x \beta_y})_i K_i \Delta \psi_i l_i \cos \theta_i \tag{27}$$

$$\mathcal{I} = 2\sum_i^8 (\sqrt{\beta_x \beta_y})_i K_i \Delta \psi_i l_i \sin \theta_i \tag{28}$$

where the sum runs over the 8 quadrupoles in the two triplets, $K_i, \Delta \psi_i, l_i$ are the strengths, roll angles, and lengths respectively of the individual quadrupoles. The phase argument is $\theta_i = [\psi_x - \psi_y - (\nu_x - \nu_y - p)\frac{s}{R}]_i$. Let $\theta_{s_1}, \theta_{s_2}$ label the corresponding phases at the skew quadrupole correctors upstream and downstream of the IP respectively. Setting the contribution to C_{diff} from the roll of the triplets to zero requires that the skew quadrupole strengths be

$$K_{s_1} = -\frac{1}{(\sqrt{\beta_x \beta_y})_{s_1} l_{s_1}} \frac{\mathcal{R} \sin \theta_{s_2} - \mathcal{I} \cos \theta_{s_2}}{\sin(\theta_{s_2} - \theta_{s_1})} \tag{29}$$

$$K_{s_2} = \frac{1}{(\sqrt{\beta_x \beta_y})_{s_2} l_{s_2}} \frac{\mathcal{R} \sin \theta_{s_1} - \mathcal{I} \cos \theta_{s_1}}{\sin(\theta_{s_2} - \theta_{s_1})} \tag{30}$$

The strengths required to correct the difference resonance $\nu_x - \nu_y = p$ depends sensitively on how the *difference* of the horizontal and vertical phases propagates through the IR. Due to the small phase advance through the IR, the imaginary component of this phasor is very small and in fact can be left uncorrected. Then a single skew quadrupole on each side of the IP can be used to correct the real part of the phasor due to the IR quadrupoles on that side [5]. The expression for the corrector strength then simplifies to

$$K_s = -\frac{1}{(\sqrt{\beta_x \beta_y})_s l_s \cos \theta_s} \mathcal{R} \tag{31}$$

Quadrupole	Maximum roll allowed $\Delta\psi_{max}$ [mrad]
Q1	7.9
Q2a	5.7
Q2b	4.4
Q3	3.5

Table 9: Maximum roll of individual quadrupoles that can be corrected with the available MCQS skew quadrupoles. Here only a single quadrupole is misaligned at a time. These skew quadrupole strengths are calculated by cancelling the contribution to the strength of the difference resonance from the rolled quadrupole.
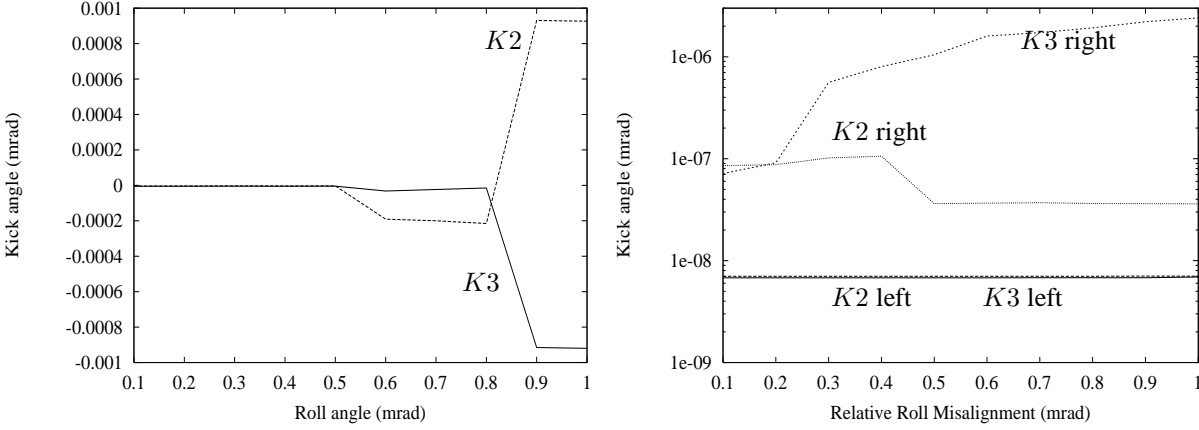

Figure 25: Absolute strength of MCBX dipole layers vs relative roll angle. These correctors only correct the orbit through the IP but not the coupling. Left: Only Q2b is misaligned. Up to 1mrad of roll, very little of the corrector strengths are used. The MCBX dipole strengths are therefore not the source of roll tolerances for Q2a/Q2b. Right: Q2a is rolled in the opposite direction to Q2b. Here the corrector strengths are essentially zero.

As a reference starting point in calculating the phases we use the upstream end of Q3 furthest away from the IP.

The maximum gradient and length of the skew quadrupoles in MCQS are 22T/m and 0.4m respectively [8]. Using these values and equation (31), we have calculated the maximum roll for each quadrupole that can be corrected, assuming that it is the only quadrupole that is misaligned. Table 9 shows the values.

There are 2^8 different possibilities for the distribution of the sign of the roll angle amongst the 8 quadrupoles in the triplets. Assuming that the signs are uncorrelated, the allowed rms roll angle per quadrupole is $\sigma_{roll} = \sqrt{\sum_i \Delta\psi^2_{i,max}}/N = 2.8$mrad. In practice, this will be too large an rms roll angle to allow. Operation with various machines has shown that for the diagnostics to make sense, coupling before correction should be limited so that the minimum tune split is no greater than 0.05. Applying this criterion to all sixteen high beta triplet quadrupoles in an rms sense requires that the rms roll angle before correction should be less than 0.3mrad.

The above criterion on the allowed roll angle can be relaxed for a Q2a/Q2b pair using the principle of self compensation. A relative misalignment between Q2a and Q2b can be corrected without a skew quadrupole by splitting the angle between these quadrupoles and rolling Q2a in the opposite direction. A calculation in Appendix B shows that coupling effects are exactly compensated with this scheme. Furthermore Figure 25 shows that the orbit is also corrected since the required corrector strengths are negligibly small.

The dynamic aperture has been calculated with a relative roll of 1mrad between Q2a and Q2b. The two quadrupoles were rolled in opposite directions by 0.5mrad. Figure 26 shows that the dynamic aperture with these self-compensating rolls is about the same everywhere in configuration space compared to the case without any misalignments. This is
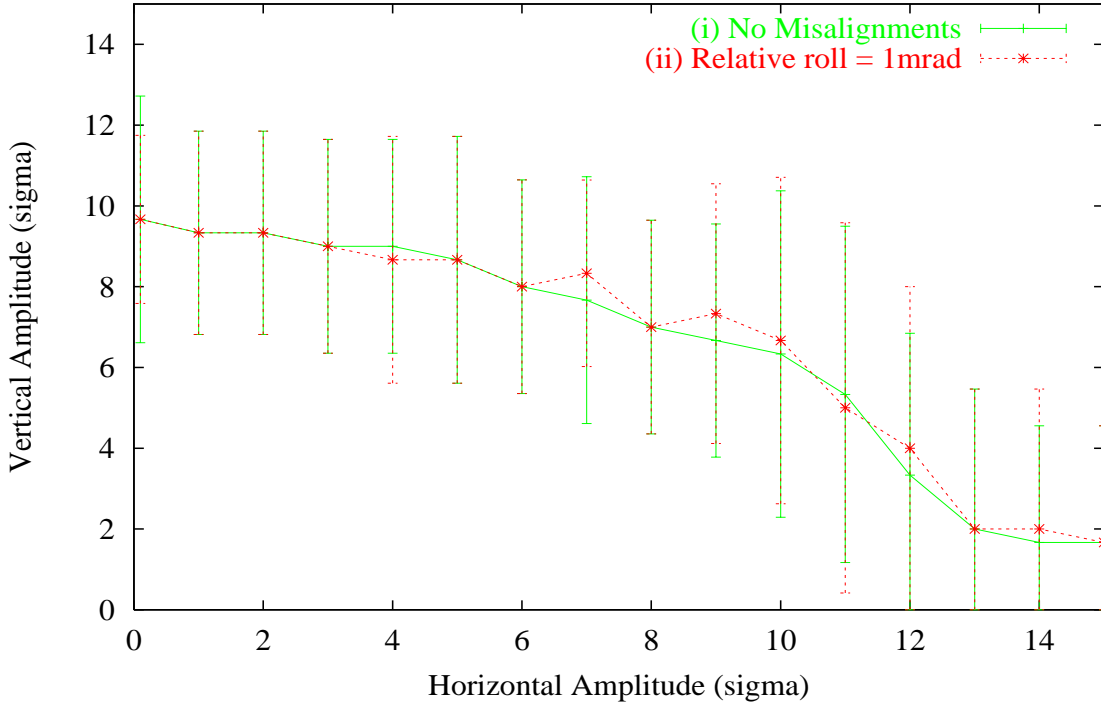
24

Figure 26: Dynamic aperture when the relative rotational misalignment between Q2a and Q2b is 1mrad. The two cases shown correspond to: (i) no misalignments, (ii) Q2a and Q2b are rolled by 0.5mrad in opposite directions about the longitudinal axis. In each case three random seeds are used for the multipole errors. This figure shows that the relative misalignment of 1mrad does not affect the dynamic aperture significantly.

confirmed by the result in Table 10 which shows that the dynamic aperture averaged over three seeds and configuration space is the same in both cases. Our results both on the coupling compensation and dynamic aperture show that equal and opposite rolls of 0.5mrad in Q2a and Q2b have no impact on the dynamics. It is possible that even larger relative roll angles may have no significant impact on the dynamic aperture but we have not confirmed this. We believe that it should be possible to mechanically align the two quadrupoles with a relative roll of less than 1mrad.

Relative roll: $\Delta\psi$ [mrad]	Average Dynamic aperture $\langle DA \rangle \pm \sigma_{\langle DA \rangle}$
None	11.2 ± 1.8
1.0	11.2 ± 1.8

Table 10: The average dynamic aperture calculated over 3 random seeds and 16 angles in coordinate space with and without roll misalignments. On each side of IP5, Q2a and Q2b were given equal and opposite roll angles of 0.5mrad. There is no observable consequence on the dynamic aperture.

5 All misalignments present

It is likely that when the cold masses of Q2a and Q2b are placed in the common cryostat, they will be misaligned in more than one degree of freedom. We have seen earlier that when Q2a and Q2b are misaligned individually in a single degree of freedom such as to provide compensating kicks, the dipole correctors are barely used. A more stringent test of the self compensation would be to misalign these quadrupoles in more than one degree of freedom. In this section we will examine the impact of transverse offsets, pitch, yaw and roll misalignments simultaneously in all four Q2a/Q2b pairs in the high luminosity IRs 1 and 5. The orbit will be corrected within the IRs as before and we will calculate the dynamic aperture. In Section 2.3 we showed that there are three ways to choose the sign of the transverse offsets [cf. Figure 10] within an IR. In this section we will choose the sign that enhances the effects of the misalignment, viz. case (iii), such that the closed orbit in the crossing plane is further away from the magnetic center of Q2b on both sides of the IP. This ensures that alignment tolerances we derive from this study are the most conservative possible.

MAD was used to find the ratios of the misalignments in Q2a and Q2b such that their effects on the orbit are self compensated and require minimal use of the correctors. The settings shown in Table 11 are found to be optimal.

	Left	Right
Transverse offsets	$\Delta x(Q2a) = -1.05\Delta x(Q2b)$	$\Delta x(Q2a) = -1.21\Delta x(Q2b)$
	$\Delta y(Q2a) = -1.21\Delta y(Q2b)$	$\Delta y(Q2a) = -1.05\Delta y(Q2b)$
Pitch	$\Delta\phi(Q2a) = -1.1\Delta\phi(Q2b)$	$\Delta\phi(Q2a) = -0.985\Delta\phi(Q2b)$
Yaw	$\Delta\theta(Q2a) = -1.08\Delta\theta(Q2b)$	$\Delta\theta(Q2a) = -0.997\Delta\theta(Q2b)$
Roll	$\Delta\psi(Q2a) = -\Delta\psi(Q2b)$	$\Delta\psi(Q2a) = -\Delta\psi(Q2b)$

Table 11: Optimal ratios of compensating alignments of the Q2a/Q2b pair on either side of the IP. With these settings, the dipole corrector strengths are minimized and the orbit is well corrected through the IP.

Figure 27 and 28 show the corrected orbit through IR5 with the misalignments shown. It is clear from Figure 28 that increasing the relative pitch angle to 0.5mrad increases the vertical distortion significantly. A similar statement is true for the effect of the yaw on the horizontal orbit in IR1. These suggest that it would be advisable to keep the pitch and yaw misalignments around 0.1mrad. Corrector strengths required are about 1% of their maximum strengths even with multipole errors. Appendix D shows the average strengths required with five different seeds for the multipole errors. It is clear that with these self compensating misalignments in all five degrees of freedom, the MCBX correctors can be used to correct mainly for the misalignments of Q1 and Q3.

The dynamic aperture with all the misalignments of Q2a and Q2b has been calculated with a larger sampling, 10 seeds, of random errors. Figure 29 shows the dynamic aperture for the three cases described in the caption. We observe that the misalignments do not affect the dynamic aperture significantly.

Misalignments			Average DA	Average difference	Largest drop in DA
$\Delta x_{rel}, \Delta y_{rel}$ [mm] Case (iii)	$\Delta\theta_{rel}, \Delta\phi_{rel}$ [mrad]	$\Delta\psi_{rel}$ [mrad]	$\langle DA \rangle \pm \sigma_{\langle DA \rangle}$	seed to seed	over 10 seeds
None			11.9 ± 1.6	-	-
1.0, 1.0	0.1, 0.1	1.0	11.9 ± 1.6	-0.003	-0.4
0.5, 0.5	0.1, 0.1	1.0	12.0 ± 1.6	0.05	-0.2
1.0, 1.0	0.5, 0.5	1.0	11.8 ± 1.6	-0.08	-0.8

Table 12: The average dynamic aperture calculated over 10 random seeds and 16 angles in coordinate space with and without all misalignments. All four Q2a/Q2b pairs in the high luminosity IRs 1 and 5 were misaligned. The worst case (iii) [cf. Figure 10] for the transverse offsets corresponds to those settings in which the closed orbit is further away from the magnetic center of the quadrupole where the β function is larger.

Table 12 shows the average dynamic aperture for these cases and an additional fourth case with the relative pitch and yaw increased to 0.5mrad. The average in all these cases is about the same. However for the fourth case, the largest drop in dynamic aperture amongst the 10 seeds is nearly 1σ which is significant. This confirms our earlier estimate that pitch and yaw misalignments should be kept below 0.5mrad, preferably close to 0.1mrad. Relative transverse offsets up
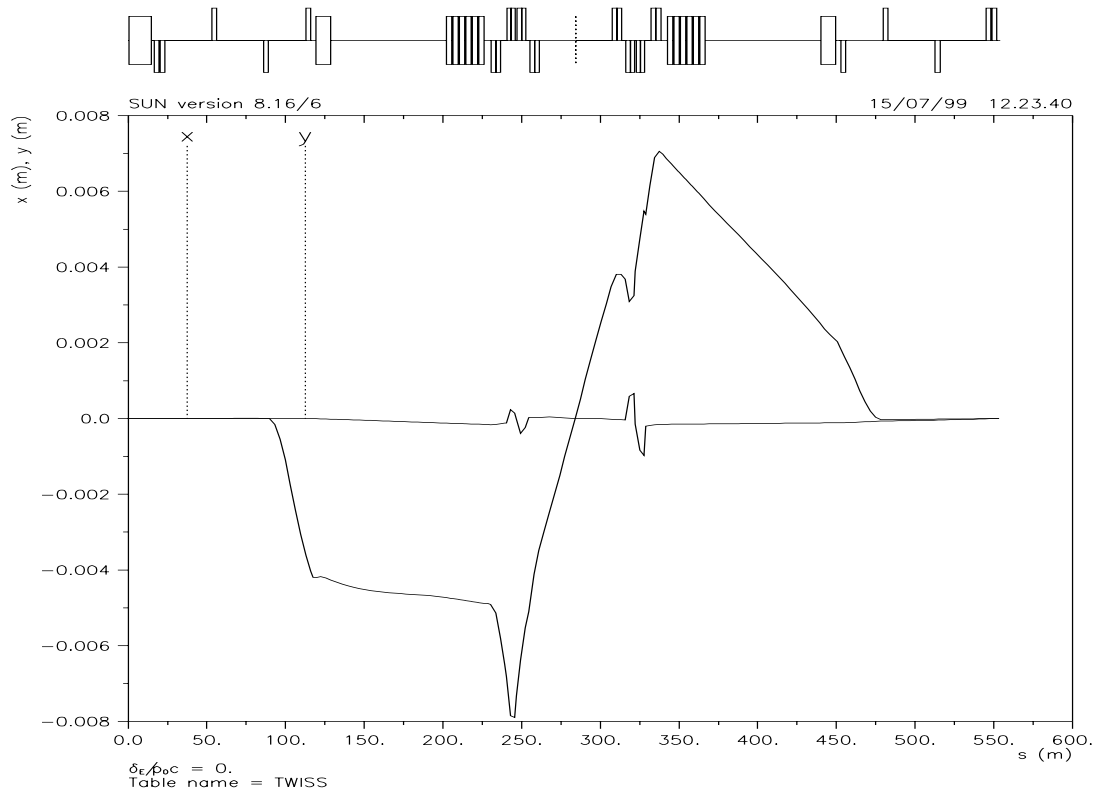
Figure 27: Orbit through IR5 with relative misalignments between Q2b and Q2a of $\Delta x_{rel} = \Delta y_{rel} = 1.0$ mm, $\Delta\phi_{rel} = \Delta\theta_{rel} = 0.1$mrad, $\Delta\psi_{rel} = 1$mrad.
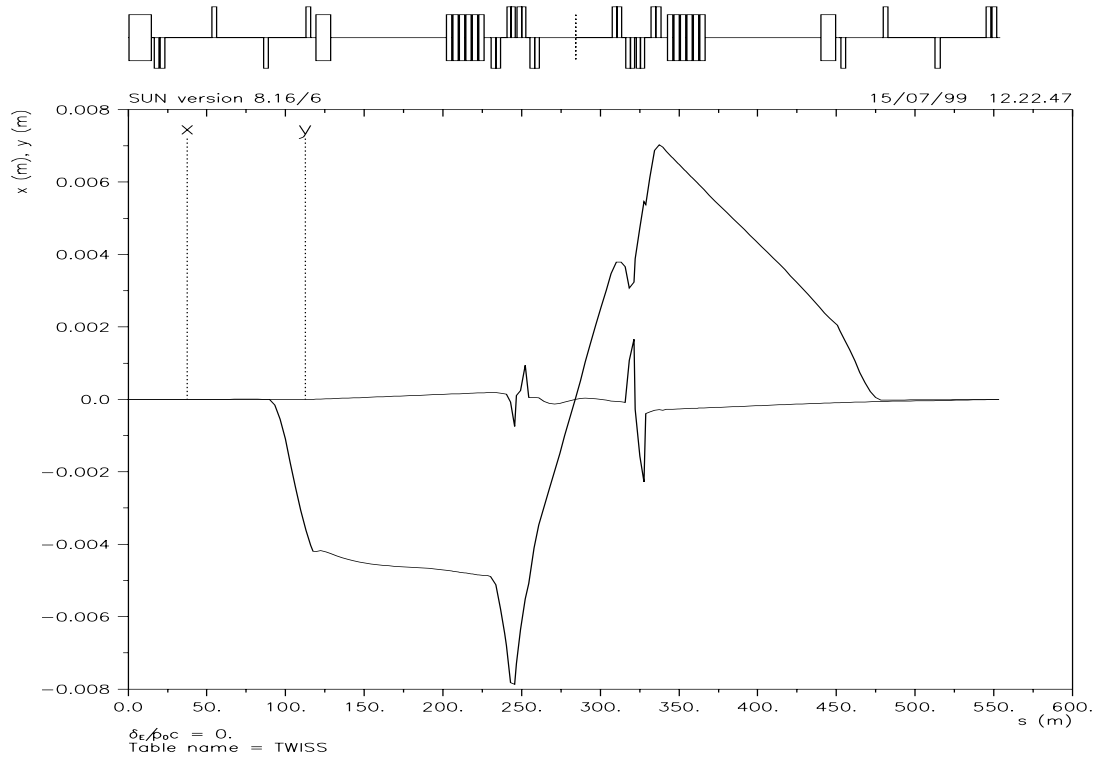

Figure 28: Orbit through IR5 with offset and roll misalignments between Q2b and Q2a the same as in Figure 27. Pitch and yaw misalignments increased to $\Delta\phi_{rel} = \Delta\theta_{rel} = 0.5$mrad. Here the vertical orbit distortion due to the pitch is significantly greater suggesting that pitch and yaw misalignments should be kept below 0.5mrad.
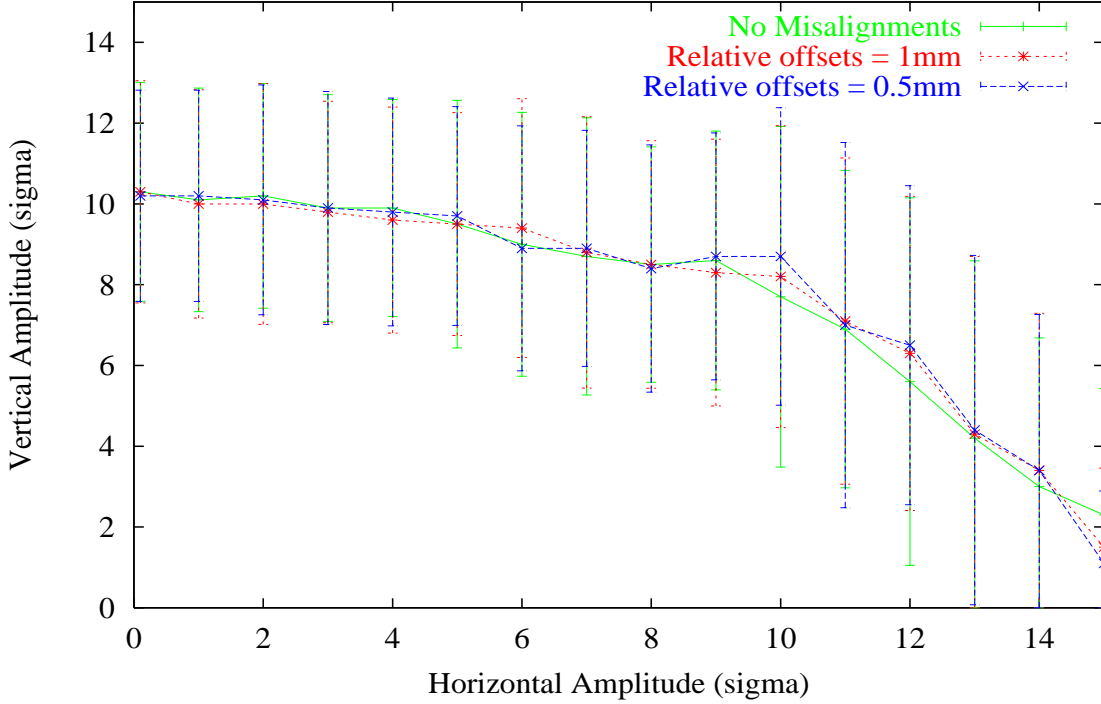
Figure 29: Dynamic aperture with and without all misalignments. Particles are tracked for 1024 turns with aperture restrictions at ±30mm in the triplets located in IR1 and IR5. The average dynamic aperture and the rms deviations over 10 random seeds for the multipole errors are shown. All four Q2a/Q2b pairs in IR1 and IR5 are misaligned. The misalignments include transverse offsets in both planes, pitch, yaw and roll. Relative pitch and yaw of 0.1mrad, relative roll of 1mrad.

to 1.0mm and relative roll up to 1.0mrad in all four pairs of Q2a/Q2b in the high luminosity IRs appear to be tolerable.

6 Summary

Alignment errors of the triplet quadrupoles cause closed orbit shifts and have a direct impact on the luminosity. Without any closed orbit correction for the misalignments, the tolerances for all misalignments, except longitudinal placement, are orders of magnitude smaller what is feasible. Closed orbit corrections to correct for these misalignments are absolutely essential.

The closed orbit shifts due to the quadrupoles Q2a and Q2b can be done in two different ways. The first would simply use the dipole windings in the MCBX corrector packages to correct for their individual misalignments. The maximum allowable misalignments are the values at which the full strengths of the correctors are used. Assuming that the misalignments of the quadrupoles in a triplet are uncorrelated and all have the same tolerances, we arrive at the tolerances shown in Table 13.

Transverse displacements	Pitch and yaw	Roll
0.27mm	0.1mrad	0.3mrad

Table 13: RMS alignment tolerances with orbit correction using the dipole correctors but without self-compensation. The rms roll angle is determined by requiring that the rms minimum tune split from all high beta quadrupoles before correction equals 0.05.

However a more efficient way would take advantage of the fact that Q2a and Q2b would be welded together in

a common cryostat so the effects of a relative misalignments between these quadrupoles can to a large extent be cancelled by misaligning the cryostat as a whole. The desired offsets and angles of the cryostat would depend on the relative misalignments and larger relative misalignments can therefore be tolerated. Table 11 summarizes the ratios of the misalignments of Q2a and Q2b that lead to minimal orbit perturbations. With these settings the dipole correctors in MCBX are not really needed (as seen in Table D.1 in Appendix D) in order to maintain well centered collisions at the IP.

We have examined the impact of these misalignments on the dynamic aperture. With all four Q2a/Q2b pairs in IR1 and IR5 misaligned in all degrees of freedom except longitudinal translation, we obtain the relative tolerances between Q2a and Q2b shown in Table 14. If these tolerances are met and the common cryostat can be aligned as desired to

Transverse displacements	Pitch and yaw	Roll
0.5mm	0.1mrad	1mrad

Table 14: Relative alignment tolerances between Q2a and Q2b with orbit and coupling compensation from self-compensating misalignments of Q2a and Q2b. Dipole and skew quadrupole correctors are used at minimal strengths. Strictly speaking, the relative roll angle of 1mrad is not an upper bound as larger roll angles may also not have a significant impact on the dynamics. These tolerances are calculated assuming that the common cryostat can be aligned exactly as desired.

maintain the self compensation, there should be no significant impact on the luminosity or beam dynamics.

However there will be errors in aligning the common cryostats to their desired positions so the self compensation will not be perfect. The relative alignment tolerances of Q2a and Q2b therefore may need to be tighter than those stated in Table 14. Given that there are relative misalignments between Q2a and Q2b, we assume that during installation, the worst case would correspond to one quadrupole, say Q2a, being perfectly aligned with the common magnetic center and Q2b being completely misaligned. In this case the misalignment of Q2b is not compensated at all. The orbit correctors on either side must be able to correct the orbit due to misalignments (presumed uncorrelated) of three quadrupoles. Assuming that all have the same alignment tolerance, the relative alignment tolerance between Q2a and Q2b in this worst case scenario is $\sqrt{4/3}\Delta T$ where ΔT is the appropriate tolerance from Table 13. The impact of these misalignments may be further mitigated by the proposal to mount the IR quadrupoles on movable jacks [1] and beam based alignment techniques.

References

[1] S. Weisz, LHC Project Note 59 (1996)

[2] J. Kerby, private communication

[3] H. Grote and C. Iselin, The MAD Program, CERN/SL/90-13 (AP)

[4] J.-P. Koutchouk, *Requirements of beam dynamics on the alignment of the low-beta insertions*, IR alignment workshop, FNAL, Oct 4-5, 1999

[5] J.-P. Koutchouk, private communication

[6] T. Sen, unpublished notes

[7] G. Parzen, Proc. PAC 1991, pg 1872

[8] A. Ijspeert and M. Karppinen, *Corrector Engineering challenges and issues*, BNL IR Corrector Workshop, May 5-6, 1999
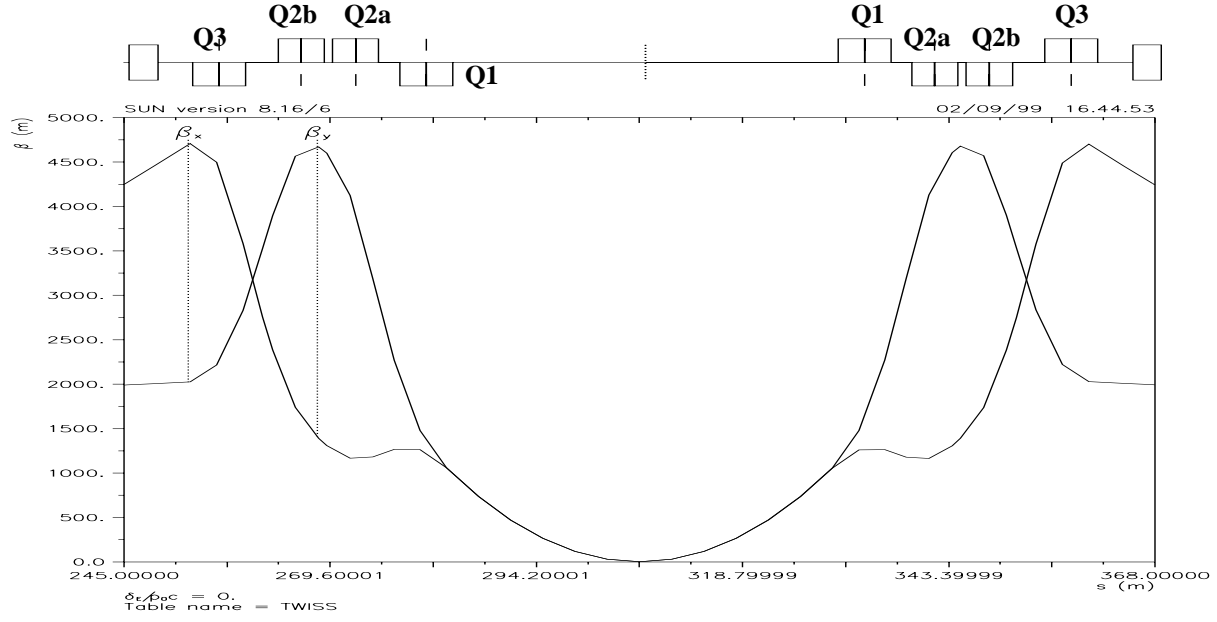
Figure A.1: Beta functions within the triplet quadrupoles upstream and downstream of the IP.

A Appendix: Optics functions in the triplets

Figure A.1 shows the beta functions within the triplets in the high luminosity IRs. Tables A.1 and A.2 shows the beta functions and dispersion respectively in the two planes at various locations within the triplet quadrupoles downstream of the IP.

Name	(β_x, β_y)[m]/(σ_x, σ_y)[mm]		
	Beginning	Middle	End
Q1	(1058.5, 1058.5)/(0.729, 0.729)	(1263.6, 1478.2)/(0.797, 0.862)	(1264.3, 2271.2)/(0.797, 1.068)
Q2a	(1180.2, 3188.1)/(0.770, 1.266)	(1165.5, 4124.6)/(0.765, 1.440)	(1306.9, 4601.9)/(0.810, 1.521)
Q2b	(1391.3, 4673.3)/(0.836, 1.532)	(1739.6, 4567.0)/(0.935, 1.515)	(2385.3, 3898.1)/(1.095, 1.399)
Q3	(3578.9, 2832.8)/(1.341, 1.193)	(4494.5, 2218.2)/(1.503, 1.056)	(4704.6, 2026.0)/(1.536, 1.009)

Table A.1: Beta functions at various locations within the quadrupoles downstream of the IP

Name	(D_x, D_y)[m]		
	Beginning	Middle	End
Q1	(-0.695, 0)	(-0.761, 0)	(-0.762, 0)
Q2a	(-0.737, 0)	(-0.733, 0)	(-0.777, 0)
Q2b	(-0.802, 0)	(-0.898, 0)	(-1.053, 0)
Q3	(-1.291, 0)	(-1.448, 0)	(-1.482, 0)

Table A.2: Dispersion functions at various locations within the quadrupoles downstream of the IP
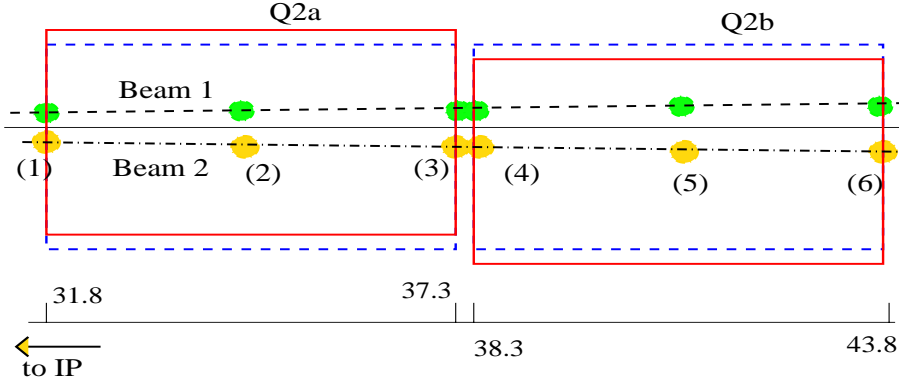
31

Figure B.1: Sketch of the closed orbit of both beams in the crossing plane through Q2a and Q2b with and without transverse offsets. The locations (2) and (5) are in the middle of quadrupoles.

B   Appendix: Physical aperture with transverse offsets

Here we will consider the change in physical aperture of both beams when Q2a and Q2b are offset in opposite directions by 0.5mm. There is a possible loss of physical aperture in the case that the offsets are in the plane of the crossing angle and we consider this case. The beam pipe radius in both Q2a and Q2b is 30mm. The closed orbit is obtained using MAD assuming a half crossing angle of 150μrad.

Beam 1

Location	Distance from IP [m]	Closed orbit [mm]	Physical Aperture - aligned [mm]	units of σ	Physical Aperture - with $\pm$0.5mm offset [mm]	units of σ
(1)	31.80	3.644	26.356	20.8	26.856	21.2
(2)	34.55	3.621	26.379	18.3	26.879	18.7
(3)	37.30	3.835	26.165	17.2	26.665	17.5
(4)	38.30	3.956	26.044	17.0	25.544	16.7
(5)	41.05	4.424	25.576	16.9	25.076	16.6
(6)	43.80	5.181	24.819	17.7	24.319	17.4

Beam 2

Location	Distance from IP [m]	Closed orbit [mm]	Physical Aperture - aligned [mm]	units of σ	Physical Aperture - with $\pm$0.5mm offset [mm]	units of σ
(1)	31.80	5.988	24.012	19.0	23.512	18.6
(2)	34.55	6.811	23.189	16.1	22.689	15.8
(3)	37.30	7.194	22.806	15.0	22.306	14.7
(4)	38.30	7.250	22.750	14.8	23.250	15.2
(5)	41.05	7.167	22.833	15.1	23.333	15.4
(6)	43.80	6.622	23.378	16.7	23.878	17.1

Table B.1: Physical aperture of both beams with and without transverse offsets of $\pm$0.5mm in the plane of the crossing angle.

Table B.1 shows that the physical aperture increases in one quadrupole and decreases in the other quadrupole for both beams. The largest reduction in physical aperture is about 0.4σ which is less than the 1σ loss considered acceptable [1].
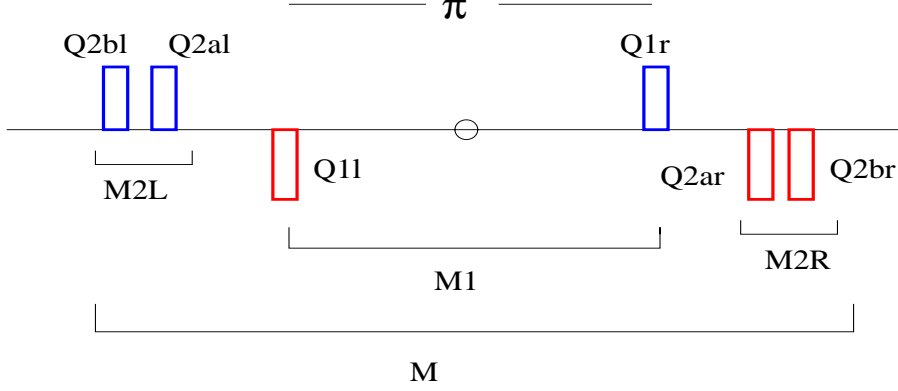
Figure C.1: Transfer matrices from a Q2 pair on the left of the IP to the Q2 pair on the right.

C Appendix: Removal of local coupling by opposite rotational angles

Roll of one of the triplet quadrupoles produces significant coupling due to the large β functions. Here we show that the coupling caused by a roll angle ψ in Q2b may be exactly compensated by an opposite roll angle of $-\psi$ in Q2a. We demonstrate this by proving that the off-diagonal terms of the transfer matrix vanish.

We will assume zero phase advance between the Q2a and Q2b forming a pair. If Q2a and Q2b on the left in Figure C.1 are rolled by angles ϕ_a^L, ϕ_b^L respectively, the transfer matrix M_{2L} between the pair is

$$M_{2L} = \begin{bmatrix} 1 & 0 & 0 & 0 \\ -q_2(\cos(2\psi_a^L) + \cos(2\psi_b^L)) & 1 & -q_2(\sin(2\psi_a^L) + \sin(2\psi_b^L)) & 0 \\ 0 & 0 & 1 & 0 \\ -q_2(\sin(2\psi_a^L) + \sin(2\psi_b^L)) & 0 & q_2(\cos(2\psi_a^L) + \cos(2\psi_b^L)) & 1 \end{bmatrix} \tag{C.1}$$

where q_2 is the inverse focal length, assumed equal for both quadrupoles. Locally coupling is removed if $\psi_b^L = -\psi_a^L$ but there is a small change in focusing given by $(1 - \cos 2\psi)q_2 \sim O(\psi^2)$.

The phase advance between Q1 upstream of the IP to the Q1 downstream is assumed to be π. The transfer matrix M_1 between these quadrupoles is

$$M_1 = -I$$

independent of the strength of Q1. M_{2R}, the transfer matrix between the Q2 pair on the right, is similar to M_{2L} but with the sign of q_2 changed.

The transfer matrix M over the section shown in Figure C.1 is $M = M_{2R}M_1M_{2L}$ and is explicitly given by,

$$M = \begin{bmatrix} -1 & 0 & 0 & 0 \\ -q_2(\cos(2\psi_a^R) + \cos(2\psi_b^R) - \cos(2\psi_a^L) - \cos(2\psi_b^L)) & -1 & M_{41} & 0 \\ 0 & 0 & -1 & 0 \\ q_2(\sin(2\psi_a^L) + \sin(2\psi_b^L) - \sin(2\psi_a^R) - \sin(2\psi_b^R)) & 0 & -M_{21} & -1 \end{bmatrix} \tag{C.2}$$

This transfer matrix and hence that of the entire ring is invariant under the roll angles if

$$\cos(2\psi_a^R) + \cos(2\psi_b^R) - \cos(2\psi_a^L) + \cos(2\psi_b^L) = 0 \tag{C.3}$$
$$\sin(2\psi_a^L) + \sin(2\psi_b^L) - \sin(2\psi_a^R) - \sin(2\psi_b^R) = 0 \tag{C.4}$$

This can be done by choosing e.g.

$$\psi_a^L = \psi_a^R, \qquad \psi_b^L = \psi_b^R \tag{C.5}$$
$$\psi_a^L = -\psi_b^L, \qquad \psi_a^R = -\psi_b^R \tag{C.6}$$

If we require that the change in focusing vanish identically, equation C.5 must hold, i.e. both Q2a quadrupoles must be rolled in the same direction and by the same amount and similarly for Q2b. If we only require that the coupling vanish, then it is sufficient to fulfill only equation C.6, i.e. the Q2 pair on each side must be rolled by equal and opposite amounts.

D   Appendix: Dipole corrector strengths with all misalignments

The corrector strengths required when all four Q2a/Q2b pairs in IR1 and IR5 are misaligned with transverse offsets, pitch, yaw and roll angles are shown in Table D.1. The values shown are averaged over 5 random seeds for the multipole errors.

Corrector	IR1		IR5		Max. value [mrad]
	Left	Right	Left	Right	
K2	0.876E-5	0.108E-3	0.383E-3	0.253E-3	0.56E-1
K3	0.876E-3	0.109E-3	0.528E-3	0.944E-4	0.56E-1
K4[hkick]	0.907E-3	0.370E-3	0.104	0.0506	0.156
K4[vkick]	0.0489	0.105	0.140E-2	0.146E-2	0.156

Table D.1: IR corrector dipole strengths required to correct the orbit with relative misalignments of Q2a, Q2b equal to $\Delta x_{rel} = \Delta y_{rel} = 1$mm, $\Delta\phi_{rel} = \Delta\theta_{rel} = 0.5$mrad, $\Delta\psi_{rel} = 1.0$mrad. The corrector strengths shown are the averages over 5 random seeds for the multipole errors. The strengths have the same sign in each case and the variations about the averages are small. The labelling of the correctors is shown in Figure 4. It is evident that with the self-compensating misalignments of each Q2 pair, the correctors are used at very low strengths.

From the values shown in this table, it is clear that the K4 dipoles required to create the crossing angle stay at close to their usual values while the other dipoles K2 and K3 are required at less than 1% of their maximum strengths. These dipoles K2 and K3 in the MCBX corrector packages can therefore be used to primarily correct the orbit due to misalignments of the Q1 and Q3 quadrupoles.